Contrôle non linéaire de robots sphériques non holonomes à des fins d'exploration spatiale

par

Aminata Ndeye Ndambao DIOUF

MÉMOIRE PAR ARTICLES PRÉSENTÉ À L'ÉCOLE DE TECHNOLOGIE SUPÉRIEURE
COMME EXIGENCE PARTIELLE À L'OBTENTION DE LA MAÎTRISE AVEC MÉMOIRE EN GÉNIE AÉROSPATIALE
M. Sc. A.

MONTRÉAL, LE 16 NOVEMBRE 2023

ÉCOLE DE TECHNOLOGIE SUPÉRIEURE
UNIVERSITÉ DU QUÉBEC

PRÉSENTATION DU JURY

CETTE THÈSE A ÉTÉ ÉVALUÉE

PAR UN JURY COMPOSÉ DE:

M. David St-Onge, directeur de mémoire
Département de génie mécanique à l'École de technologie supérieure

M. Saad Maarouf, codirecteur
Département de génie électrique à l'École de technologie supérieure

Mme Ornwipa Thamsupan , président du jury
Département de génie mécanique à l'École de technologie supérieure

M. Jean-Philippe Roberge, membre du jury
Département de génie des systèmes à l'École de technologie supérieure

M. Georges Ghazi, membre du jury
Département de génie des systèmes à l'École de technologie supérieure

ELLE A FAIT L'OBJET D'UNE SOUTENANCE DEVANT JURY ET PUBLIC

LE 07 NOVEMBRE 2023

À L'ÉCOLE DE TECHNOLOGIE SUPÉRIEURE

REMERCIEMENTS

Je souhaite exprimer ma profonde gratitude envers le professeur David St-Onge pour sa confiance en moi dans le cadre de ce projet, ainsi que pour son précieux encadrement, son soutien inestimable et sa disponibilité tout le long de l'élaboration de mon mémoire.

Je tiens aussi à exprimer ma reconnaissance envers le professeur Maarouf Saad, mon co-directeur de recherche, pour son soutien constant durant ce projet. Ses conseils avisés ont grandement enrichi mon travail.

J'aimerais également remercier Bruno Belzile, Yassine Kali et Simon Bonneau pour leur assistance, ainsi que tous les membres du laboratoire INIT Robots pour l'environnement de travail favorisant l'épanouissement, la collaboration et une ambiance positive.

Un grand merci à l'INSA Haut-de-France ainsi qu'à l'ETS qui m'ont permit de réaliser ce double diplôme. Je suis reconnaissante pour les ressources et les opportunités qu'elles m'ont offertes.

Ma famille mérite toute ma reconnaissance pour son soutien constant et son encouragement sans faille. Mes frères Aliou, Ousseynou, Youm et Mbissane, mon oncle et mentor Mbissane Diouf, ainsi que ma précieuse sœur Maimouna ont toujours été à mes côtés, ont cru en moi dès le début et ont fourni des efforts inlassables pour contribuer à ma réussite.

À Sadikh Sow, dont la présence a été une source de réconfort et d'encouragement pendant cette période, je dis un immense merci.

Je ne saurais oublier de mentionner mes très chers amis Téné , Linda, Fatou, Nathan, Hemil et tous les autres qui se reconnaitront et qui ont été une bouée de sauvetage émotionnelle, apportant de la joie et de la motivation dans ce parcours académique exigeant.

Je souhaite tout particulièrement souligner l'importance de ma mère, Thioro DIONE et de mon defunt père Fallou DIOUF à qui je dédie ce mémoire, qui ont été ma véritable boussole tout au long de ce parcours.

Contrôle non linéaire de robots sphériques non holonomes à des fins d'exploration spatiale

Aminata Ndeye Ndambao DIOUF

RÉSUMÉ

Dans le cadre de la recherche scientifique et de l'exploration de l'inconnu, l'exploration spatiale se démarque comme l'un des domaines les plus captivants et cruciaux de notre époque. Elle fait appel à une gamme variée de véhicules spatiaux conçus pour des missions et des objectifs diversifiés. Parmi ces vehicules nous avons les rovers, des engins automatisés spécialement conçus pour se déplacer à la surface de planètes et de lunes. Des exemples notables de rovers incluent le rover Curiosity sur Mars et le rover Perseverance.

Cependant, les rovers présentent des limitations intrinsèques, telles qu'une vitesse de déplacement très lente, des environnements hostiles susceptibles de réduire leur durée de vie, une capacité limitée à transporter des instruments scientifiques, ainsi que des terrains difficiles qui peuvent entraver leurs déplacements.

Face à ces défis, les robots sphériques se présentent comme une alternative prometteuse pour l'exploration spatiale. Ils se distinguent par leur capacité à combiner la vitesse, la résistance aux collisions et l'efficacité, tout en nécessitant un nombre minimal d'actionneurs.

Il existe plusieurs types de robots sphériques, chacun se distinguant par sa méthode d'actionnement. Dans le cadre de cette étude, nous nous concentrons sur les robots sphériques barycentriques (BSRs), qui se déplacent en ajustant leur centre de masse, en mettant particulièrement en lumière ARIES, un robot sphérique à 2 degrés de liberté spécialement conçu pour l'exploration de cavernes sur la lune.

L'objectif de cette recherche réside dans la modélisation d'ARIES en utilisant la méthode de Lagrange, en adoptant trois approches distinctes : une approche simplifiée, supposant que les mouvements transversaux et longitudinaux sont indépendants, une approche complète, sans simplification aucune et une approche visant la réduction de la dynamique du système. Parallèlement, nous explorons le contrôle d'ARIES en utilisant le contrôle par mode glissant, tout en procédant à une validation par comparaison avec le contrôle par couple calculé. Nous comparons aussi le mécanisme d'ARIES à celui d'un pendule double qui est plus courant dans la littérature.

Les résultats obtenus révèlent que le contrôle par mode glissant offre des performances remarquables pour des systèmes tels qu'ARIES. Parallèlement, ils mettent en évidence que la dynamique complète procure des performances supérieures comparé aux autres dynamiqes en terme de précision.

Cette étude apporte une contribution significative à notre compréhension des robots sphériques, de leur modélisation à leur contrôle. Ces résultats sont appelés à guider le développement futur

de robots sphériques et à éclairer les choix de conception et de contrôle dans un large éventail d'applications.

Mots-clés: robots spheriques, contrôle par mode glissant, Lagrange, modélisation dynamique, réduction de la réticence

Nonlinear Control of Non-Holonomic Spherical Robots for Space Exploration

Aminata Ndeye Ndambao DIOUF

ABSTRACT

In the realm of scientific research and exploration of the unknown, space exploration stands out as one of the most captivating and crucial fields of our time. Space exploration involves a diverse range of spacecraft designed for various missions and objectives. Among these vehicles, rovers are automated machines specifically designed to traverse the surfaces of planets and moons. Notable examples of rovers include the Curiosity rover on Mars and the Perseverance rover.

However, rovers have inherent limitations, such as slow movement speed, exposure to hostile environments that can reduce their lifespan, limited capacity for carrying scientific instruments, and challenging terrains that can hinder their mobility.

In the face of these challenges, spherical robots emerge as a promising alternative for space exploration. Their integration into the aerospace domain has become a significant focus over the past decade. They stand out for their ability to combine speed, collision resistance, and efficiency while requiring a minimal number of actuators.

There are several types of spherical robots, each distinguished by its method of actuation. In this study, we focus on barycentric spherical robots (BSRs), which move by adjusting their center of mass, with particular emphasis on ARIES, a 2-degree-of-freedom spherical robot specially designed for lunar cave exploration.

The goal of this research lies in modeling ARIES using the Lagrange method, adopting three distinct approaches : a simplified approach assuming independent transverse and longitudinal movements, a complete approach without any simplifications, and an approach aimed at reducing the system's dynamics. Concurrently, we explore the control of ARIES using sliding mode control, while validating it through comparison with computed torque control. We also compare ARIES' mechanism to that of a double pendulum, a more common concept in the literature.

The results reveal that sliding mode control offers remarkable performance for systems like ARIES. Additionally, they highlight that the complete dynamics yield superior performance, even though decoupled dynamics reduce the number of parameters and, consequently, computation time.

This study makes a significant contribution to our understanding of spherical robots, spanning from their modeling to their control. These findings are poised to guide the future development of spherical robots and inform design and control choices across a wide range of applications.

Keywords: Spherical Robots, Sliding Mode Control, Lagrange, Dynamic Modeling Chattering reduction

TABLE DES MATIÈRES

Page

LISTE DES TABLEAUX

Page

LISTE DES FIGURES

Page

LISTE DES ABRÉVIATIONS, SIGLES ET ACRONYMES

ARIES	Autonomous robotic intelligent explorer sphere
ASC	Agence Spatiale Canadienne
ASE	Agence Spatiale Européenne
BSR	Barycentric spherical robots
COAM	Conservation of the angular momentum
DOF	Degree-of-freedom
ETS	École de Technologie Supérieure
IMU	Inertial measurement unit
RMSE	Root mean square error
ROS	Robot Operating System
SLR	Systematic litterature review
SRR	Spherical rolling robots
SLR	Systematic Literature Review
UWB	Ultra Wide Band

LISTE DES SYMBOLES ET UNITÉS DE MESURE

A	Ampère
cm	Centimètres
g	Grammes
J	Joules
Kg	Kilogrammes
m	Mètres
m/s^2	Mètre par seconde carré
m^2	Mètres carrées
N	Newton
rad	Radians
rad/s	Radian par seconde
s	Secondes
W	Watts

INTRODUCTION

Au fil des décennies, l'exploration spatiale a été le vecteur par lequel l'humanité a poussé les frontières de sa compréhension et de sa technologie pour s'aventurer dans les régions les plus reculées de l'espace, révélant ainsi les mystères des mondes lointains, les phénomènes cosmiques énigmatiques, et les secrets de notre propre planète, le tout sous un nouveau prisme : l'exploration spatiale. Au cœur de cette exploration spatiale, la Lune, notre satellite naturel, occupe une place particulièrement importante. Récemment, elle a suscité un regain d'intérêt avec le succès de la mission chinoise Chang'e 4, qui a marqué le premier alunissage historique sur la face cachée de la Lune en janvier 2019. La Lune elle-même abrite des caractéristiques géologiques uniques à sa surface, connues sous le nom de "puits lunaires". Ces puits lunaires, en plus d'être des énigmes géologiques fascinantes, offrent un potentiel extraordinaire pour la recherche spatiale, car ils pourraient abriter des cavités souterraines qui pourraient servir de refuges pour les futurs explorateurs lunaires ou révéler des découvertes scientifiques remarquables.

Cependant, ces cavités souterraines restent un mystère, et il est impératif de les explorer pour en comprendre la nature et les opportunités qu'elles pourraient offrir. Les rovers traditionnels, bien que remarquables, présentent des limitations en termes de taille, d'autonomie, et de capacité à naviguer dans des terrains difficiles, ce qui rend leur utilisation dans de tels environnements complexe.

C'est là qu'interviennent les robots sphériques. Leur conception unique les rend idéaux pour l'exploration spatiale. Leur petite taille permet d'en envoyer un essaim pour contourner les problèmes d'autonomie. Ils sont protégés par une coque sphérique, ce qui garantit la sécurité de leur mécanique et de leurs systèmes embarqués dans des environnements hostiles. Enfin, leur capacité à se déplacer de manière omnidirectionnelle les rend extrêmement agiles, même dans des terrains difficiles. De plus, la plupart d'entre eux sont capables de transporter des charges

utiles significatives, telles que des lidars, des caméras, et d'autres capteurs, ce qui en fait des outils précieux pour la recherche spatiale.

Dans ce contexte, est né le projet de conception d'un robot sphérique novateur, nommé ARIES (Autonomous Robotic Intelligent Explorer Sphere), en réponse à un appel d'offres de l'Agence Spatiale Européenne. ARIES se distingue par son joint cylindrique unique agissant comme un pendule à l'intérieur de sa coque sphérique, une innovation protégée par un brevet. La finalité du projet est d'avoir une flotte d'ARIES (six au total) capables de faire de la localisation ainsi qu'une cartographie des cavernes. Cette flotte pourra être deployé grâce à un robot spécialement conçu pour cela. La figure 0.1 met en contexte le projet ainsi que son objectif.

Figure 0.1 Description du projet ARIES. L'image en arrière plan vient du site de l'agence spatiale européenne : *Lunar Caves exploration*

Le premier robot sphérique a vu le jour en Finlande, à l'université d'Helsinki Halme, Schonberg & Wang (1996) en 1995. Sa conception visait à lui permettre d'évoluer dans des environne-

ments extrêmes. Depuis lors, de nombreux chercheurs se sont penchés sur cette catégorie de robots, qui se distinguent considérablement des robots conventionnels par leur forme et leur mode de déplacement. Les robots sphériques, grâce à leur coque protectrice de mécatronique, sont particulièrement adaptés à l'exploration d'environnements hostiles.

Parmi les différents types de robots sphériques, le plus courant est le robot sphérique barycentrique, qui utilise le déplacement de son centre de masse pour se mouvoir. D'autres exploitent la conservation du moment angulaire grâce à un volant d'inertie, par exemple, pour générer le couple nécessaire au déplacement. Certains robots sphériques tirent parti des propriétés de leur coque pour se déplacer.

La dynamique d'un robot sphérique peut sensiblement différer de celle des robots conventionnels en raison de facteurs tels que sa forme sphérique, les interactions avec le sol, et la répartition de la force ou du couple, qui influent tous sur son mouvement. Le développement d'un modèle dynamique précis s'avère donc être une étape cruciale avant d'aborder le contrôle de ces systèmes robotiques. Dans le cas d'ARIES, cette modélisation est complexifiée par la présence de contraintes non holonomes, ce qui signifie que les mouvements transversaux et longitudinaux du robot ne sont pas indépendants.

Pour mener à bien ce projet, nous avons réalisé une revue de littérature systématique, examinant les différentes conceptions de robots sphériques, les méthodes de modélisation et de contrôle employées. Bien que la méthode de Lagrange soit la plus couramment utilisée, d'autres approches, telles que les méthodes de Newton, de Kane, et l'identification des systèmes, présentent chacune leurs avantages et inconvénients. Cette analyse a également permis d'identifier divers défis liés aux robots sphériques, notamment les limitations liées à leurs points de contact, l'intégration de capteurs supplémentaires, l'évitement d'obstacles, et le contrôle de systèmes non holonomes. Parmi les 33 méthodes de contrôle recensées pour les robots sphériques, le contrôle par mode glissant s'est révélé être le plus performant et le plus largement utilisé. Ces conclusions nous

ont conduit à sélectionner la méthode de modélisation et de contrôle pour ARIES, utilisant la méthode de Lagrange et un contrôle par mode glissant avancé comme dans Mozayan, Saad, Vahedi, Fortin-Blanchette & Soltani (2016).

Pour confirmer la validité du modèle et du choix du contrôleur, nous avons procédé à une série de simulations à l'aide de Simulink. Les résultats obtenus ont confirmé l'efficacité du contrôleur en termes de robustesse, de précision et d'efficacité énergétique.

Ce mémoire est organisé en plusieurs chapitres pour présenter de manière méthodique les résultats de la recherche. Il commence par le chapitre 1, qui expose les outils et les méthodes qui ont été utilisés tout au long de l'étude. Ensuite, le chapitre 2 plonge dans une revue de la littérature approfondie, se penchant sur la conception et le contrôle des robots sphériques. Cette revue de la littérature permet d'examiner l'état actuel de la recherche dans ce domaine, offrant ainsi un contexte essentiel pour la compréhension des travaux réalisés. Le chapitre 3 constitue le cœur de la thèse, se consacrant à la modélisation dynamique et au contrôle du robot sphérique ARIES. Ce chapitre explore divers modèles et modes d'actionnement, éclairant ainsi les choix effectués pour la conception et le contrôle d'ARIES. Enfin, la conclusion, synthétise les principales conclusions et découvertes de la recherche. Elle offre également des suggestions pour des pistes de recherche futures, mettant en évidence les domaines où des améliorations et des développements ultérieurs pourraient être nécessaires pour faire progresser la compréhension des robots sphériques et leur utilisation dans l'exploration spatiale et d'autres applications.

CHAPITRE 1

MÉTHODOLOGIE

1.1 Étapes de la Recherche

Pour mener à bien cette recherche, nous avons suivi une série d'étapes. Tout d'abord, nous avons identifié le problème en effectuant un examen approfondi des robots sphériques existants similaires à ARIES. Ensuite, nous avons fait une acquisition des connaissances grâce à une revue de la littérature systématique sur les conceptions et le contrôle des robots sphériques. Ces informations ont servi de base pour formuler nos questions de recherche et nos objectifs. Nous avons ensuite évalué ces questions de recherche et objectifs à l'aide de simulations sur Simulink.

1.1.1 Identification du Problème

ARIES utilise un mécanisme de propulsion distinctif. Elle est constitué d'une coque sphérique contenant un mécanisme cylindrique actionné se comportant comme un pendule. Ce mecanisme est décrit dans Belzile & St-Onge (2022b). Les articulations actionnées cylindriques sont des mécanismes avec deux degrés de liberté (rotation et translation autour du même axe). Inspiré par des travaux antérieurs, ARIES utilise deux moteurs rotatifs identiques et intègre deux vis à filetage (une à droite et une à gauche). Les moteurs se déplacent à l'intérieur de la coque sphérique en suivant l'axe de roulis du robot. La sortie de ce mécanisme génère à la fois la rotation pour faire rouler la sphère et la translation pour orienter les poulies sur un même plan. Les deux moteurs tournent à la même vitesse dans la même direction, créant une rotation pure vers l'avant, tandis que s'ils tournent en sens inverse à la même vitesse, une translation pure se produit avec une bascule de la sphère dans le plan orthogonal. Cette conception offre une variété de mouvements cylindriques en combinant ces deux mouvements de base. Le mécanisme est représenté à la figure 1.1

Étant donné cette configuration exceptionnelle, il n'existe aucun modèle dynamique établi ni de stratégie de contrôle pour les robots sphériques dotés d'un mécanisme interne similaire. Par

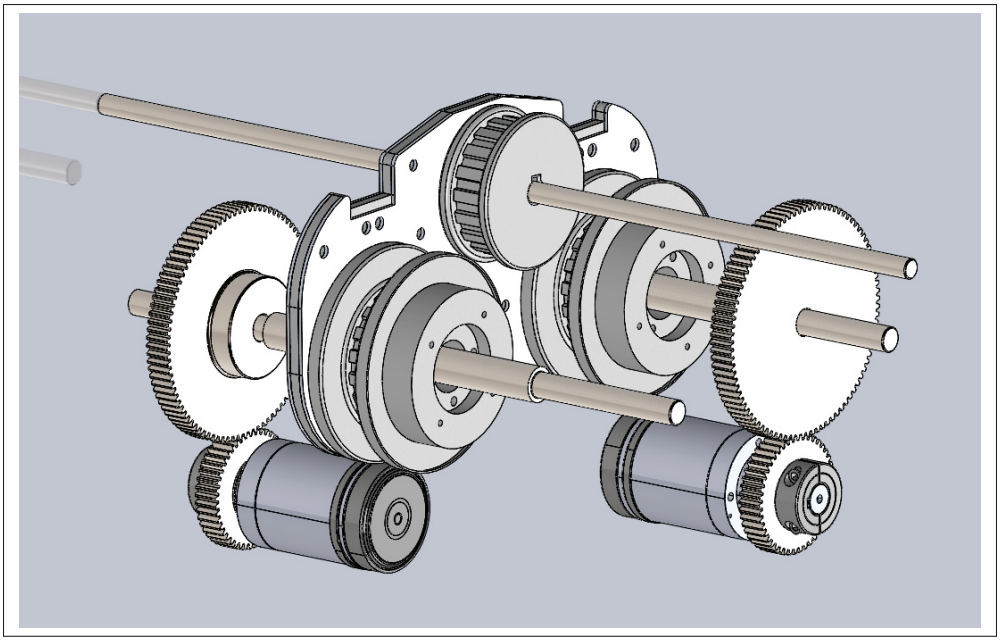

Figure 1.1 Mécanisme d'actionnement d'ARIES

conséquent, cette recherche vise à établir un modèle dynamique fondamental pour les robots sphériques partageant des dynamiques similaires et à développer une stratégie de contrôle efficace adaptée à ces robots. De plus, il convient de noter que de nombreuses études antérieures sur les robots sphériques ont adopté une approche simplifiée, en supposant l'indépendance des mouvements transversaux et longitudinaux, ce qui simplifie le modèle. Par conséquent, il est nécessaire de mener des recherches impliquant à la fois des modèles simplifiés et non simplifiés d'ARIES pour faciliter une comparaison significative des modèles dérivés.

1.1.2 Acquisition de Connaissances

Pendant cette phase, nous avons réalisé une revue approfondie de la littérature existante sur les robots sphériques, couvrant tout, de leur conception et de leurs stratégies de contrôle à la modélisation dynamique. Cette recherche nous a permis d'acquérir une compréhension approfondie de l'état actuel de la technologie des robots sphériques. Nous avons appris diverses conceptions utilisées dans les robots sphériques et les méthodes employées pour les contrôler.

De plus, nous avons recueilli des informations sur les caractéristiques importantes de ces robots, telles que leur masse, leur taille, ainsi que les capteurs et les actionneurs qu'ils utilisent.

Notre revue de la littérature a également exploré les différentes approches utilisées pour modéliser ces robots, notamment la méthodes de Lagrange, de Newton-Euler, la méthode de Kane et les techniques d'identification de système. De plus, nous avons identifié et exploré les différents défis associés à cette technologie.

1.1.3 Objectifs de Recherche et Validation

Les principaux objectifs de cette recherche englobent le développement de stratégies de contrôle robustes pour la modélisation et le contrôle d'ARIES, tout en réalisant une analyse comparative entre trois approches de modélisation dynamique distinctes : la dynamique complète,la dynamique découplée et la dynamique réduite. Pour atteindre ces objectifs de recherche, nous nous sommes appuyés sur les informations tirées de notre revue de la littérature systématique, qui a indiqué que le contrôle en mode glissant surpassait systématiquement d'autres méthodes selon divers critères, comme discuté dans le chapitre suivant. La validation des modèles dynamiques et des stratégies de contrôle implique des simulations approfondies réalisées dans Simulink.

1.2 Structure du mémoire et Contributions

Ce mémoire basée sur des articles est organisée comme suit :

- Chapitre 2, intitulé *Spherical Rolling Robots—Design, Modeling, and Control : A Systematic Literature Review*, a été soumis au journal *Robotics and Autonomous Systems*. Ce chapitre fournit une analyse approfondie de l'état actuel de l'art en matière de conception et de contrôle des robots sphériques. Les crédits d'auteur sont répartis comme suit :
  - **Aminata Diouf :** Responsable de la section sur le contrôle, recherche de publications, sélection, extraction de données, analyse et rédaction.
  - **Bruno Belzile :** Axé sur les aspects de la conception, extraction de données, analyse, rédaction et révision.

  - **David St-Onge, Maarouf Saad :** ont fourni des orientations, examiné le travail et contribué à la révision.

- Chapitre 3, qui traite de la modélisation et du contrôle d'ARIES, est intitulé *Modeling and control of a pendulum-driven spherical robot using sliding mode control*. Ce chapitre a été soumis à *The Journal of Dynamic Systems, Measurement, and Control* et fournit les étapes de la modélisation et du controle d'ARIES ainsi qu'une comparaison des différentes méthodes de modélisation mentionnées ci-dessus et une validation des modèles. Les crédits d'auteur pour ce chapitre sont attribués comme suit :
  - **Aminata DIOUF :** Responsable de la modélisation, de la programmation, des simulations, des expériences et de la rédaction.
  - **David St-Onge, Maarouf Saad :** ont offert des orientations sur la modélisation et le contrôle, participé à l'examen et contribué à la rédaction.

Enfin, le mémoire se conclura par une secion de conclusion, fournissant un aperçu de la recherche, résumant les résultats, mettant en évidence les limitations et offrant des recommandations pour les travaux futurs.

CHAPITRE 2

SPHERICAL ROLLING ROBOTS—DESIGN, MODELING, AND CONTROL: A SYSTEMATIC LITERATURE REVIEW

Aminata Diouf[1] , Bruno Belzile[1] , David St-Onge[1] , Maarouf Saad[2]

[1]Department of Mechanical Engineering, École de technologie supérieure,
1100 Notre-Dame Ouest, Montréal, Québec, Canada H3C 1K3
[2] Department of Electrical Engineering, École de technologie supérieure,
1100 Notre-Dame Ouest, Montréal, Québec, Canada H3C 1K3

Article submitted in the journal "Robotics and Autonomous Systems" in June 2023.

2.1 Abstract

Spherical robots have garnered increasing interest for their applications in exploration, tunnel inspection, and extraterrestrial missions. Diverse designs have emerged, including barycentric configurations, pendulum-based mechanisms, etc. In addition, a wide spectrum of control strategies has been proposed, ranging from traditional PID approaches to cutting-edge neural networks. Our systematic review aims to comprehensively identify and categorize locomotion systems and control schemes employed by spherical robots, spanning the years 1996 to 2023. A meticulous search across five databases yielded a dataset of 3189 records. As a result of our exhaustive analysis, we identified a collection of novel designs and control strategies. Leveraging the insights garnered, we provide valuable recommendations for optimizing the design and control aspects of spherical robots, supporting both novel design endeavors and the advancement of field deployments. Furthermore, we illuminate key research directions that hold the potential to unlock the full capabilities of spherical robots.

Keywords : Spherical robots, design, control strategies

2.2 Introduction

Spherical rolling robots (SRRs) are a fascinating category of robots characterized by their ability to move by rolling on themselves, owing to their unique spherical shape. However,

beneath this seemingly simple concept lies a plethora of sophisticated mechanisms and control strategies that enable such motion. Nearly three decades ago, NASA introduced the idea of *"Beach-Ball" Robotic Rovers* [1] for planetary exploration, igniting the exploration of various systems in this domain. Notably, the Rollo, designed in 1996 at Finland's Helsinki University of Technology Halme *et al.* (1996), stands as one of the pioneering spherical robots aimed at operating in hostile environments. The inherent protective nature of their spherical shell renders them well-suited for challenging terrains, safeguarding sensitive mechatronics, including sensors and actuators. Consequently, their applications extend to underwater exploration Lin & Guo (2012), surveys of dusty construction sites, tracking crop yields in muddy fields, and even missions in extreme environments such as the moon, Mars, and beyond Kalita, Gholap & Thangavelautham (2020); Rachavelpula (2021). Furthermore, spherical robots have also found utility in educational and therapeutic contexts, particularly for children with developmental disorders Mizumura, Ishibashi, Yamada, Takanishi & Ishii (2018); a market targeted by one of the only companies manufacturing primarily spherical robots, Sphero.

Over the years, numerous researchers and companies have proposed diverse designs, dynamic models, and control strategies for spherical rolling robots. While previous reviews exist in the literature, they fail to encapsulate the latest advancements in this field. For instance, a comprehensive examination of rolling in robotics Armour & Vincent (2006a) delves into earlier designs of SRRs, while another review Chase & Pandya (2012) focuses primarily on the different actuation mechanisms specific to spherical robots. However, since the publication of these reviews, several novel designs have emerged, necessitating an updated analysis (see Fig. 2.1). Although a recent review covered control algorithms Karavaev, Mamaev, Kilin & Pivovarova (2020), it provided limited detail on the employed control strategies due to its concise nature as a conference paper and failed to provide a holistic understanding of both mechanical and control aspects of these robots.

Figure 2.1 shows the trend in publication over the period covered in this review (1996-2023) for both mechanical design and control strategies. Since 2010, an increase in interest in SRR

[1] https ://ntrs.nasa.gov/citations/19950070425

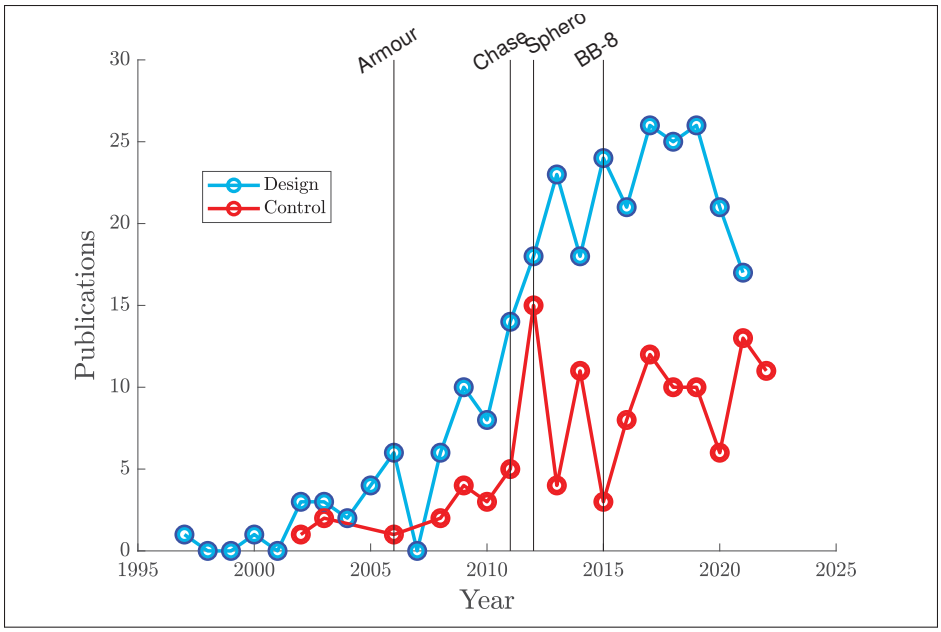

Figure 2.1 Number of publications each year on the design of SRR (blue) and their control strategies (red). The vertical lines highlight key events in the recent SRR history : the previous literature reviews from Armour (2006) and Chase (2012), the release of Sphero's first product (2011), and the first appearance of BB-8 in Star Wars movies (2015).

is observable. A common misconception is to grant this popularity to the public apparition of BB-8, a fictional spherical robot from the *Star Wars* movie franchise. However, we observe that the trend had started before that, potentially inspiring the filmmakers. We can also observe that *Sphero*'s first product release is right at the start of that new trend, around 2011.

Spherical robots feature a range of internal mechanisms that enable their movement, broadly categorized into three main groups : barycenter offset (BCO), shell transformation, and conservation of angular momentum (CoAM). Barycentric spherical robots (BSRs) manipulate the center of mass to achieve desired motion, exemplified by wheeled mechanisms within a spherical shell or popular pendulum-driven spherical robots. However, the torque capability of BSRs is constrained as the center of gravity cannot be shifted beyond the shell. This limitation can be circumvented through the utilization of control moment gyroscopes (CoAM). Conversely, shell

transformation, a less prevalent method, involves deforming the outer body of the robot using wind, air, or water to induce movement Chase & Pandya (2012).

The highly nonlinear and non-holonomic nature of spherical robots presents significant challenges in their control. Consequently, various control methods have been proposed in the literature. They most often are designed to be fully autonomous with only a few designed for teleoperation, to the extent of using brain interfaces Volosyak & Schmidt (2019); Guan *et al.* (2020). When designed for autonomy, the majority of control strategies can be achieved through nonlinear methods or local linear approximations of the system. This review will show the proportion, advantages, and disadvantages of the control strategies found in the literature of SRR, after assessing the underlying dynamic model differences.

In light of the aforementioned landscape, this paper aims to present a systematic review of spherical rolling robots, encompassing the wide range of actuation mechanisms and control strategies implemented in this domain. Through comprehensive data gathering and analysis, the review will shed light on research opportunities and identify blind spots. It is important to note that the scope of this review is limited to robotic systems utilizing their spherical shell for locomotion, as opposed to robots with a spherical shape but employing limbs. Notably, this distinction arises in numerous publications concerning amphibious and underwater spherical robots, where water jets or propellers are utilized in aquatic environments while limbs are employed on land Xing *et al.* (2020). Furthermore, this review focuses solely on active locomotion, excluding spherical robots that rely on external forces, exemplified by the NASA/JPL Tumbleweed polar rover Behar, Carsey, Matthews & Jones (2004).

The paper is structured as follows : Section 2.3 details our methodology, inspired by PRISMA, then Section 2.4 presents the extracted designs, categorized and compared, followed by Section 2.5 describing all the control strategies found in our analysis. Finally, in Section 2.7, we shed light on potential research opportunities and challenges that may unlock the full potential of SRR.

Tableau 2.1 Keywords prompt designed for each database of this literature review

Database	Keywords prompt
Compendex	(((((design OR control OR command) WN ALL) AND (("spherical Robot*" OR “spherical roll* robot*") WN ALL))) AND (english WN LA))
Web of Science	(((design OR control OR command) AND (“spheric* Robot*" OR “spheric* roll* robot*"))) Timespan : All years. Databases : WOS, CCC, DIIDW, KJD, MEDLINE, RSCI, SCIELO. Search language=Auto
Science Direct	(Design OR Control OR Command) AND (“spherical Robot” OR “spherical Robots" OR “spherical rolling robot” OR “spherical rolling robots")
Scopus	TITLE-ABS-KEY (((design OR control OR command) AND (“spheric* Robot*" OR “spheric* roll* robot*"))) AND (LIMIT-TO (LANGUAGE , “English"))
ProQuest	((design OR control OR command) AND (“spheric* Robot*" OR “spheric* roll* robot*"))

2.3 Methodology

To ensure the utmost rigor and credibility of our analysis and results, we conducted a literature review following the guidelines of the Preferred Reporting Items for Systematic Reviews and Meta-Analyses (PRISMA) framework Page *et al.* (2021). Although initially developed for medical and pharmaceutical meta-studies, PRISMA has gained traction and served as a valuable reference for various fields in recent years. In adherence to this framework, our methodology adhered to a comprehensive 27-item checklist encompassing key aspects such as methods, results, and discussions.

2.3.1 Publication search and screening

Our study encompassed all research pertaining to spherical robots, irrespective of publication year, with the caveat that the database content before 1995 is limited. Additionally, we limited our search to English and French publications. To compile our dataset, we performed thorough searches across five information sources : ProQuest, Science Direct, Web of Science, Engineering

Village, and Scopus. Employing keywords such as "design," "control," "spherical robots," and "rolling," we identified a total of 3189 records. Subsequently, through a stringent screening process, we excluded records that did not meet the predefined inclusion criteria. As a result, our study included 126 papers concerning control strategies and 280 papers addressing locomotion mechanism design.

During the eligibility assessment, we considered whether the spherical form was an integral aspect of the movement generation, thereby excluding papers where robots relied on external forces for propulsion. This criterion ensured a focused review solely on spherical robots employing their spherical shell for locomotion. To maintain an up-to-date and comprehensive analysis, we encompassed publications from 1996 (no records available before that) up until April 2023.

For each information source, the datasets utilized are presented in Tab. 2.1, providing transparency and facilitating the replicability of our search process. The study included 126 papers on control strategies for spherical robots after screening and sorting through 3189 papers obtained from various databases. The process from the start of the research to the inclusion of the 126 records is summarized in Fig. 2.2. An identical process was applied to the mechanism design topics.

2.3.2 Data extraction

The included records were exported into software for systematic literature review, which allowed for screening and data extraction. A 7-item form was created for data extraction, including questions about the control strategy used, the objectives of the control method, the outcomes of the method, the driving mechanism of the spherical robot, and whether a simulation or experiment was performed to verify the control strategy :

1. Which control strategy is used in the paper ?
2. Which dynamic modeling technique is used in the paper ?
3. What are the objectives of the control method ?
4. What are the outcomes of the method ?
5. What is the driving mechanism of the spherical robot in the study ?

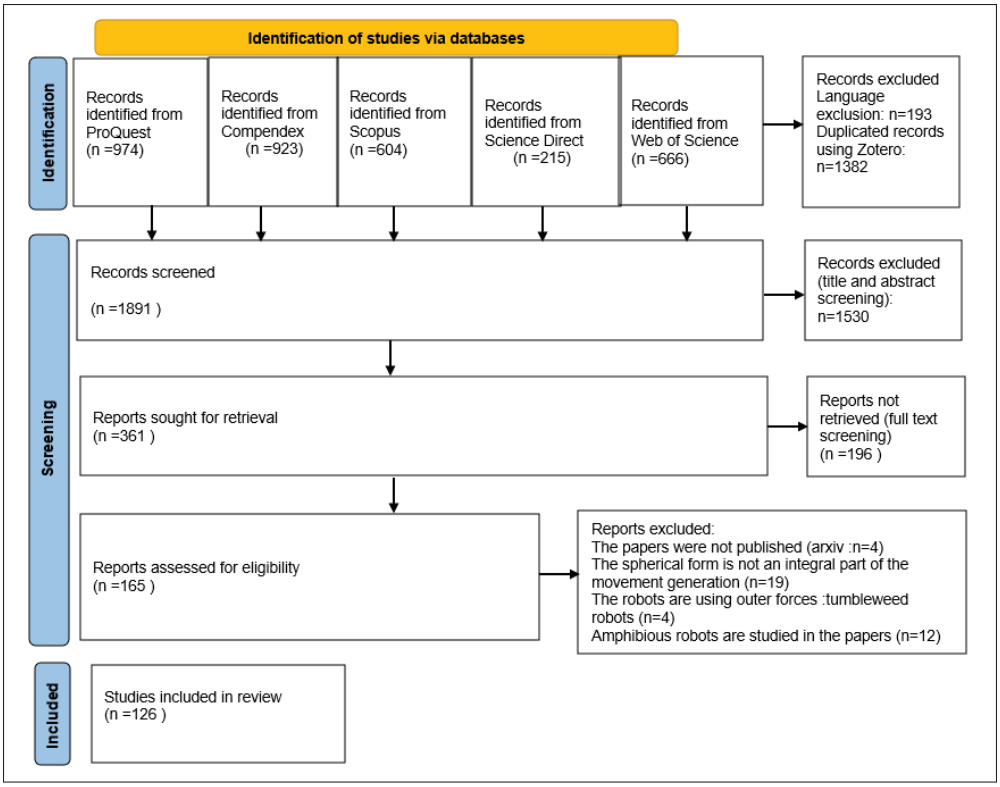

Figure 2.2 PRISMA 2020 flow diagram for new systematic reviews which included searches of databases

6. What sensors have been used or considered ?
7. Is a simulation or an experiment performed to verify the control strategy ?

Data extraction has been achieved in a redundant manner, in parallel by the first two authors. The presentation and analysis of the content extracted are covered in sections 2.4 and 2.5.

2.3.3 Bibliometric analysis of the keywords

To analyze the relationship between keywords, references from various databases were imported into VosViewer van Eck & Waltman (2017), which generated a keyword network. The final analysis included keywords that occurred more than 20 times in the papers, and 57 keywords met this threshold. Keywords with a total link strength of less than 600 were excluded from the analysis. The link strength is the strength of the relationship between the different nodes. The

most frequent keywords were "design," "spherical robots," and "control," with total occurrences of 2220, 1841, and 1643, respectively. The size of the node indicated the frequency of a keyword, while the curves represented the co-occurrence of keywords in the same publication. The distance between two nodes determined the number of co-occurrences. The shorter that distance is, the larger the number of co-occurrences will be van Eck & Waltman (2017). Figure 2.3 shows the different interactions between keywords. The analysis showed that there were more papers on the design of a spherical robot than on its control, and sliding mode control and PID were the most commonly used control strategies. The distance from the spherical robot node to the control and from the spherical robot to the design is the same as from control to design. Therefore, we can conclude that several papers address both control and design aspects, which reinforces the importance of conducting a holistic literature review like this one.

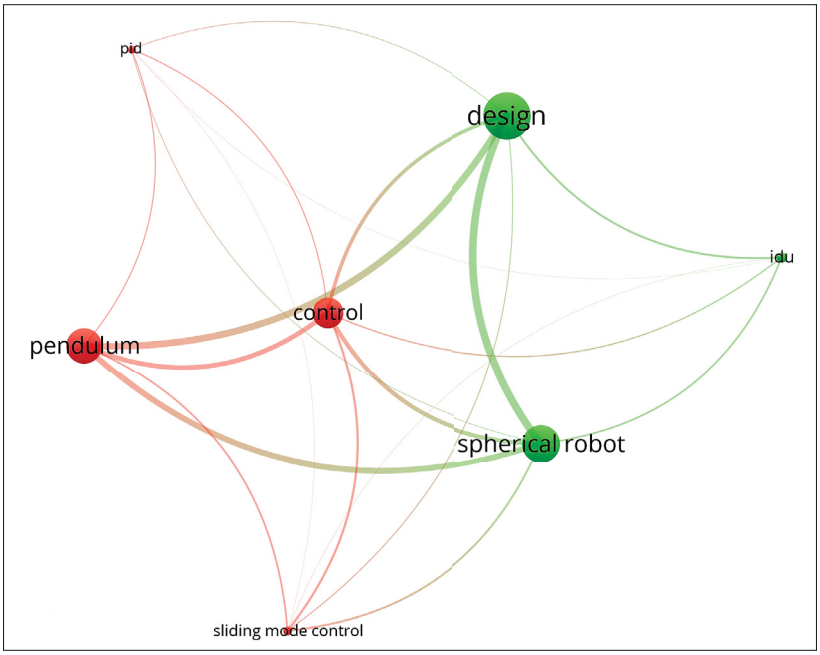

Figure 2.3 Co-occurrence analysis of the main keywords found in the publications. Made with VOSviewer

2.4 Locomotion, Design and Actuation

Our first pass on the large literature gathered focuses on their different actuation mechanisms, which will in turn define the type of system and the control variables. As shown in Fig. 2.4, the number of publications, at least partially addressing the design of the actuation mechanism of an SRR, increased significantly over the last two decades.

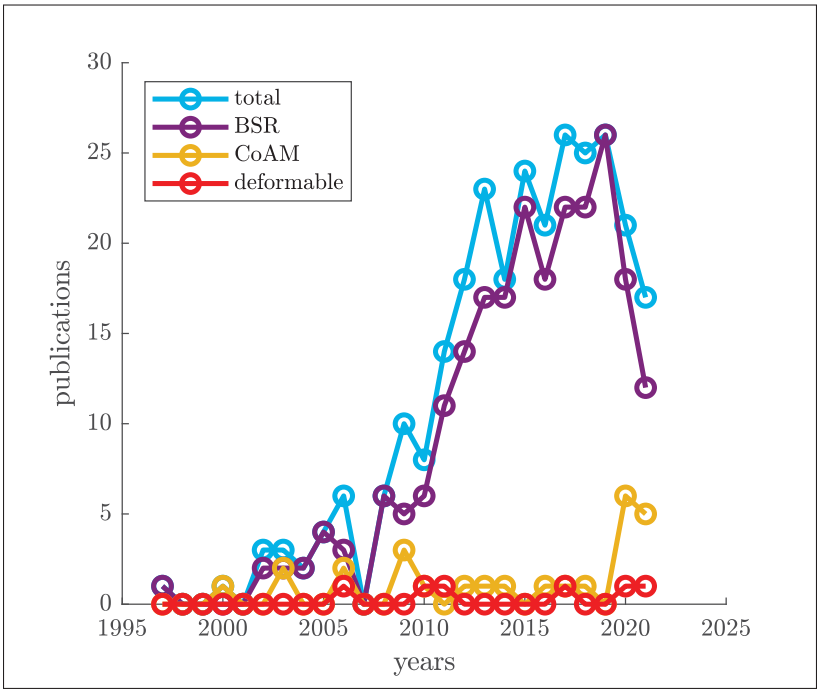

Figure 2.4 Number of included publications addressing the design of an SRR (some may appear in more than one category, having multiple driving systems)

As mentioned above, their locomotion systems can be summarized in three broad categories :

1. barycentric ;
2. conservation of the angular momentum ;
3. shell deformation.

Considering these categories, the papers identified and their corresponding devices were classified in Fig. 2.5. Since an SRR can be actuated with more than one mechanism or with a system fitting in more than one of the above three categories, the sum of robots listed in this figure is higher

than the total number of papers addressing the design of the driving mechanism. It should be noted that the BSR category was separated into subcategories in Fig. 2.5, since it is the most common type, by far. Moreover, colors used in Fig. 2.4 correspond to those of Fig. 2.5.

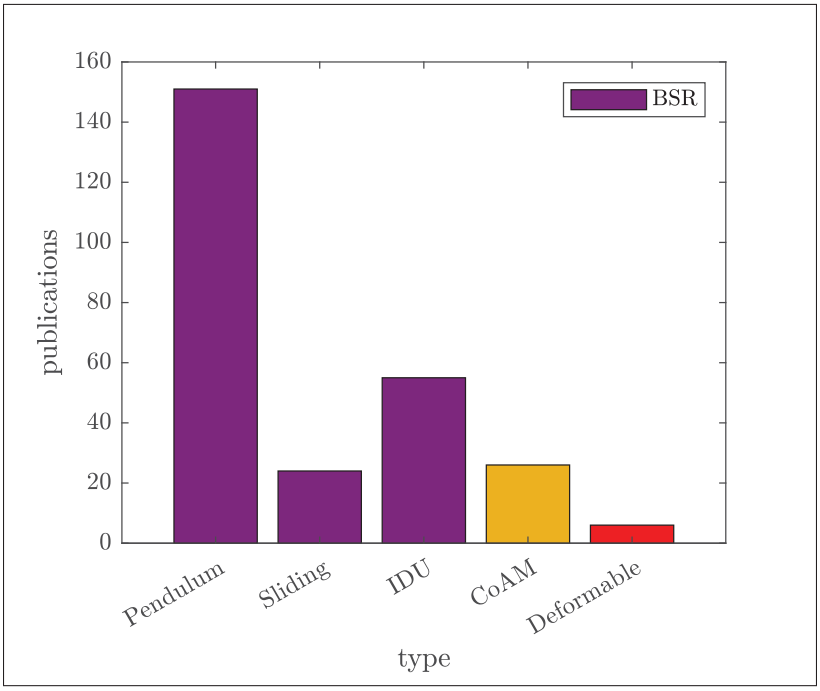

Figure 2.5 Number of design publications sorted by types of mechanism (robots with more than one actuation mechanism are counted more than once), purple for BSRs, blue for others

2.4.1 Nonholonomic motion with SRRs

Holonomic and nonholonomic motion are concepts that are frequently mentioned when it comes to mobile robots. Basically, a nonholonomic mobile robot's state depends on the path taken to reach it. In this case, the velocity constraint defining its motion is non-integral, for instance with "*rolling without slipping condition*" with wheels as they cannot slide sideways. Fundamentally, with SRRs, the spherical shape of the shell makes it capable of holonomic motion, as it can roll in any direction. However, this is typically no longer the case when we consider the internal driving mechanism. Indeed, most cannot make their external shell roll in any direction, particularly about their vertical axis. As stated by Chase and Pandya Chase & Pandya (2012), for "true

holonomy, the research challenge becomes developing an internal driving mechanism that can provide omnidirectional output torque to a sphere that can arbitrarily rotate around it, regardless of the orientation of either the sphere or the drive mechanism." This thus requires an internal driving mechanism capable of moving in three dimensions independently from the spherical shell. According to our review, this is not the case in the overwhelming majority of SSRs, with rare exceptions, which is probably motivated by the fact that holonomic motion is not necessarily needed for most situations, as it is for a car.

2.4.2 Barycentric

By far the most common type of spherical robots according to our assessment, as shown in Fig. 2.5, barycentric spherical robots (BSRs) are driven by a displacement of their center of mass (CoM). Indeed, by destabilizing the system by moving the CoM away from its point of lowest potential energy (typically directly underneath the center of rotation (CoR) of the sphere), the shell starts rolling. BSRs can be classified into several subcategories :

1. pendulum-based ;
2. IDU ;
3. sliding masses.

2.4.2.1 Pendulum-based

Among BSRs, pendulum-based BSRs are the most popular designs. The pendulum typically, but not necessarily, rotates about a shaft passing through the center of the sphere. For a robot to be able to move in more than one direction, at least two DoFs are needed. This can be done with a 2-DoF pendulum, which can rotate in two directions. Otherwise, more than one pendulum can be used. For instance, on the one hand, Li et al. Li, Deng & Liu (2009) and Zhao et al. Zhao, Li, Yu, Hu & Sun (2010) proposed BSRs with two, while on the other hand, Dejong et al. DeJong, Karadogan, Yelamarthi & Hasbany (2017), four, to increase their maneuverability. This is obviously done at the expense of more complex control schemes. Moreover, multiple pendulums do not need to be fully independent of each other. For instance, Asiri et al. Asiri,

Khademianzadeh, Monadjemi & Moallem (2019) added a second, smaller pendulum orthogonal to the main pendulum rotating about their spherical shell's main axis. Otherwise, to steer its single-pendulum BSR, Schroll Schroll (2009) designed and patented a differential mechanism to tilt the bob in a direction orthogonal to the rolling motion. While the main axle (passing through the center of the sphere with both extremities rigidly attached to the spherical shell) is usually used as the axis of the pendulum(s), it is not always the case, as demonstrated by Zhao et al. Zhao *et al.* (2010) which used circular guides carved into the ellipsoid [2] shell of its device. However, having a pendulum only attached to the shell at two places makes it easier to use a flexible shell, as shown by Ylikorpi et al. Ylikorpi, Halme & Forsman (2017). This characteristic is valuable to overcome small obstacles or steps with a reduced impact on the trajectory, while also attenuating the oscillation due to the nature of a pendulum's motion. Regardless of the number of pendulums and their designs, the rolling torque of a pendulum-based spherical robot is bounded by the diameter of its shell and the mass of its pendulum. Even if the actuator inside the sphere is capable of generating a larger torque, it will only result in the spinning of the pendulum about its axis, which is not the desired behavior. Moreover, this torque limit is also proportional to the gravitational acceleration. To increase the distance between the center of the sphere and the CoM, many authors located the battery powering their robot in the lowest part of their pendulum, as done by Landa and Pilat Landa & Pilat (2015).

While most pendulum-driven robots are incapable of holonomic motion, some have omnidirectional capabilities, notably, the four-pendulum BSR proposed by DeJong et al. DeJong *et al.* (2017). In this particular case, this is possible because the four pendulums have four different skew axes intersecting at the center of the sphere.

An example of a pendulum-based spherical robot, known as ARIES, is depicted in Figure 2.6. The robot incorporates an actuated cylindrical joint that serves as a pendulum. This novel design allows for simultaneous rolling and steering by utilizing a continuous differential transmission.

[2] For the sake of this review, papers presenting rare rolling robots with slightly ellipsoid shapes were considered, as they behave mostly as spherical robots and their actuation and control scheme can be applied to a perfectly spherical robot

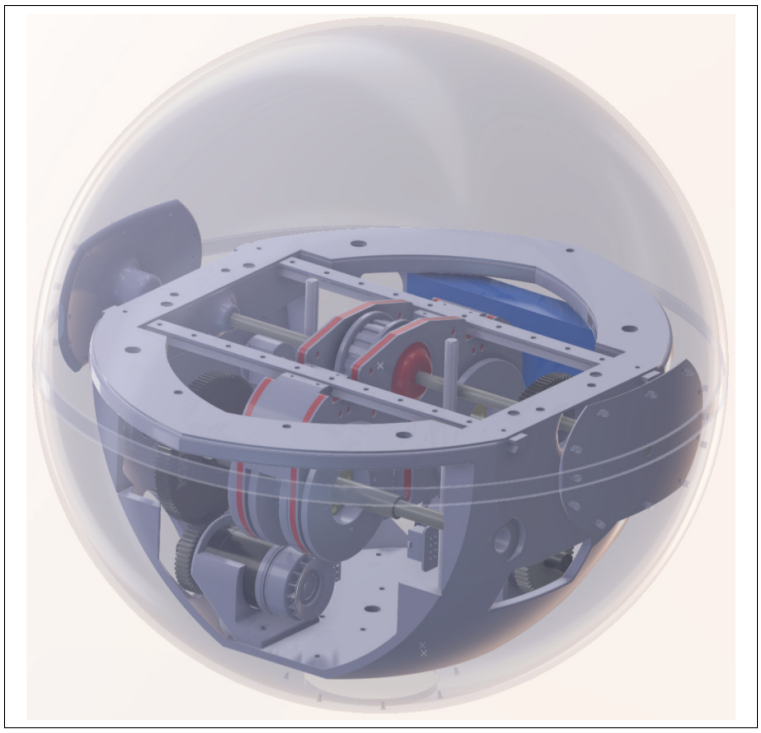

Figure 2.6 ARIES : a pendulum-based spherical robot

2.4.2.2 Internal drive unit

Another type of BSR is those with an internal drive unit. Here, a torque is transmitted to the outer shell through wheels in contact with its internal surface. Sometimes considered separately from IDUs, the *hamster ball* system defines the combination of a spherical shell and a smaller wheeled robot inside the sphere, such as the one proposed by Alves and Dias Alves & Dias (2003). In fact, this type of actuation is among the earliest examples of SRR because of its simplicity. Obviously, the potential holonomy of a *hamster-ball* SRR is linked directly to the holonomy of the internal robot. Recently, Belskii et al. Belskii, Serykh & Pankratev (2021) proposed an omnidirectional IDU to be used inside a spherical robot. This concept was not fully tested however inside a shell.

Hamster balls suffer from a major issue, namely slipping between the shell and the wheels. To overcome this limitation, IDUs generally incorporate a system to apply a force on the wheel, reducing the risk of slipping. For example, Zhan et al. Zhan, Cai & Yan (2011) developed the

concept of an omnidirectional IDU with two wheels based on the concept of barycenter offset. Their device consists of a smaller wheel used to orient a larger one in contact with the internal surface of the shell, allowing holonomic motion. Yet, these systems are still known to suffer from slipping between the internal drive and the spherical shell Chase & Pandya (2012), limiting their robustness.

2.4.2.3 Sliding masses

Finally, some BSRs use sliding masses to control the location of the CoM Mukherjee, Minor & Pukrushpan (1999); Bowkett, Burkhardt & Burdick (2017). For instance, Javadi & Mojabi (2002) used masses moving along prismatic joints to modify the location of the CoM.However, they are generally, more difficult to control than the two other subcategories described above. Indeed, in the case of masses moving linearly Javadi & Mojabi (2002), a continuous variation of the position of the masses is required, even moving in a single direction, contrary to pendulum-driven robots. This can be overcome by masses moving along circular guides, as Tafrishi et al. Tafrishi, Svinin, Esmaeilzadeh & Yamamoto (2019) did when they investigated the potential of a fluid-based BSR. They used masses moving inside pipes to control the location of the CoM thus generating motion. However, this system was not experimentally validated by the authors. As motors can generally be used as generators to accumulate energy, this is also true with spherical robots. Indeed, in applications/environments where minimizing energy consumption is critical, recharging the battery may be useful, as is the case with the robot developed by Zhai et al. Zhai, Ding, Liu, Jin & Kang (2020). The latter harvests energy while the robot is pushed by the wind with electromagnets moving along pipelines. This system can be used to actuate the robot by controlling the position of the magnets instead of letting them move according to the dynamics of the system.

2.4.3 Conservation of the angular momentum

Instead of moving the CoM for the rolling motion, another spherical robot design is to leverage the conservation of the angular momentum without having to displace the CoM. The rolling

motion is generated using reaction wheels Bhattacharya & Agrawal (2000); Joshi & Banavar (2009); Muralidharan & Mahindrakar (2015) or control moment gyroscopes (CGM) Schroll (2010); Chen, Ye, Sun & Jia (2017). The latter can provide more torque than the former, taking advantage of gyroscopic precession. However, the torque output is not continuous, contrary to the former. Moreover, reaction wheels must be fixed to the shell, rendering the mechanical design and the control challenging Muralidharan & Mahindrakar (2015). Chase Chase (2014) partially overcame this limitation by using four CGMs mounted in dual-scissored pairs.

One of the main differences between BSRs and those based on the conservation of the angular momentum is the non-continuous torque generated for the rolling motion.

2.4.4 Shell deformation

Last but not least, other types of locomotion based on deformable shells are also possible. As can be seen in Fig. 2.5, they are far less common than barycentric and angular-momentum-based SRRs. This category includes shape-memory alloys and pressurized air bladders Wait, Jackson & Smoot (2010). Their deformable spherical shell can increase maneuverability, as shown by Sugiyama and Hirai Sugiyama & Hirai (2006) with their robot capable of crawling and jumping. Generally able of holonomic motion with a basic controller, they can be complex to design and more prone to failure (i.e. unprotected moving parts).

2.4.5 Types and number of actuators

Most of the mechanisms discussed before can be actuated by different means, namely steppers, servos, brushless, etc. We tried to extract the most common types of actuators from the papers studied, unfortunately, only a few papers provide this level of detail on their prototype. Among them, Chowdhury et al. Chowdhury, Soh, Foong & Wood (2018b) utilized two Faulhaber DC gear drive motors, each with 30mNm/3V, to control a 90-gram spherical robot. Similarly, Belzile & St-Onge (2022a) used two Maxon EC 45 flat 30W brushless motors with corresponding controllers to actuate a 10kg spherical robot. They justified this choice based on the motors'

lightweight nature and their ability to fit within the limited available space. In contrast, Azizi and Keighobadi Azizi & Keighobadi (2014) proposed a design with three motors driving three independent rotors. Similarly, Jia et al. Jia, Zheng, Sun, Cao & Li (2009) proposed a design with three independent actuators, including one drive motor, one steer motor, and one flywheel. The spinning flywheel enabled increased angular momentum of the spherical robot. In Roozegar & Mahjoob (2017), two stepper motors were used as actuators, where one rotated the main shaft and the other enabled the rotation of the pendulum. Additionally, four gears were utilized for power transmission. In a different approach, Zheng, Hu & Sun (2021) employed three separate motors in the internal mechanism : a flywheel motor for increasing angular momentum, a long-axis motor for generating driving forces, and a short-axis motor for controlling the counterweight's angle relative to the shell's axis.

2.4.6 Design scale

The papers examined in this study featured spherical robots of different scales, e.g. weight and dimensions. Figure 2.7 visually represents the masses and radii of the described robots, where such information was available. It is worth noting that some authors, as observed in Yue & Liu (2012); Yue, Liu, An & Sun (2014a), employed the same spherical robot in multiple papers. To ensure accuracy, we considered each robot only once, resulting in a total of 58 distinct robots represented in the figure.

Among the examined robots, the lightest variant, proposed in Niu *et al.* (2014), weighed a mere 55 grams, while the heaviest robot, documented in Zhai, Li, Luo, Zhou & Liu (2015), weighed a substantial 50 kilograms. The analysis revealed that the majority of the examined robots weighed less than 10 kg, which can be attributed to their primary usage in exploration scenarios. The benefits of lighter robots are twofold : they require less energy to operate and are more manageable for transportation purposes.

Furthermore, the investigation into the papers unveiled that the majority of the robots possessed a radius ranging between 0.1 and 0.2 meters, with the largest radius belonging to the device

proposed by Rigatos, Busawon, Pomares & Abbaszadeh (2019), measuring 1.2 meters. In contrast, the smallest robot introduced by Nguyen et al. Nguyen, Soh, Foong & Wood (2017), exhibited a radius of 30 cm. At this scale, the onboard computer and sensing capacity are inherently limited, imposing constraints on the robot's capabilities.

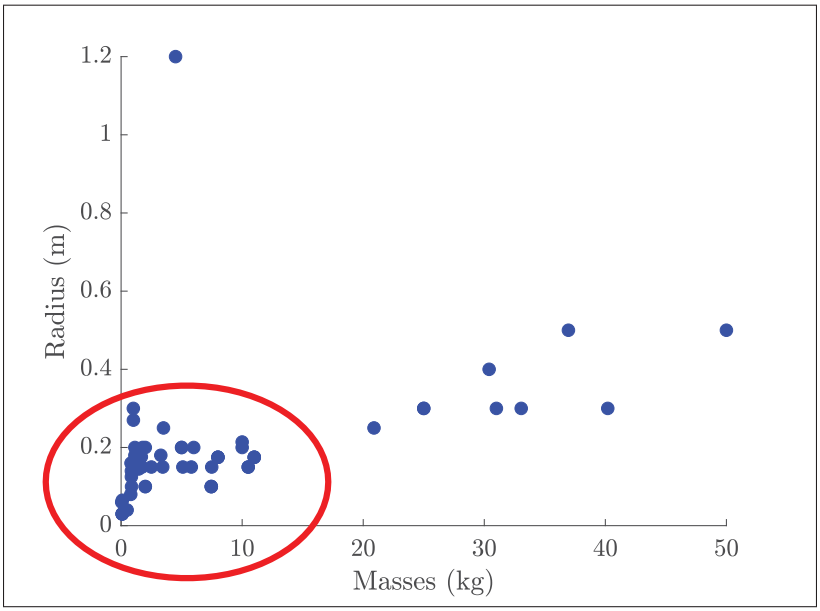

Figure 2.7 Radius and mass of included mechanisms

2.5 Control and dynamics

During our thorough analysis of the wide array of publications encompassed in this study, our subsequent phase focused on an examination of the diverse range of control strategies. In this context, Fig. 2.8 illuminates a significant trend : the emergence of publications focusing on the control of spherical robots began gaining prominence around 2012, culminating in a notable peak in 2019.

2.5.1 Dynamic modeling

Spherical robots possess a distinctive motion mechanism, resulting in intricate kinematics and dynamics to model and analyze. The incorporation of non-holonomic constraints, as discussed

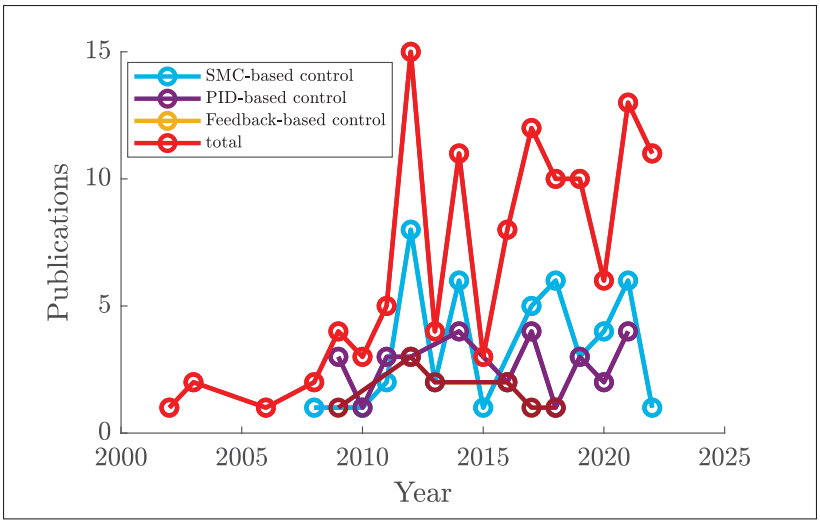

Figure 2.8 Number of papers addressing the control of an SRR following the most used control strategies

in Section 2.4.1, further amplifies the complexity of these models. While certain papers, such as Nam, Lee, Choi, Kim & Lee (2019); Li & Zhan (2018, 2019), rely solely on the kinematic model for controlling spherical robots, most studies employ a dynamic model due to the influence of conservative forces, such as the pendulum gravity effect. However, when feasible, the kinematics-only control approach offers a simplified depiction of the system's behavior, emphasizing motion or positional characteristics rather than intricate dynamics.

The dynamics of a spherical robot can deviate from those of traditional robots due to factors such as the shape of the spherical body, ground interactions, and force or torque distributions, all of which impact its motion. Developing a dynamic model is a crucial step prior to delving into the control of robotic systems. In this research, various methods were employed to model spherical robots.

Figure 2.9 illustrates the most commonly utilized techniques for modeling spherical robots. The Euler-Lagrange method is extensively employed in numerous papers for deriving the dynamic model. This method provides a systematic approach by considering the system's energy and serves as a valuable tool in modeling mechanical systems. However, the presence of motion constraints may require the use of Lagrange's multipliers, which in turn adds an additional computational

burden for calculating the corresponding constraint forces. The Newton-Euler method, widely utilized in robotics, physics, control systems, and other fields requiring accurate dynamic modeling, offers explicit equations of motion and a recursive formulation, enabling detailed analysis and control of complex mechanical systems. Its explicit representation of inter-body forces facilitates structural analysis of all the components. Alternatively, system identification techniques can be employed to create mathematical models describing a system's behavior based on input-output relationships, rather than relying on a physics-based representation. This successful strategy has been implemented in Kamaldar, M.J. & H. (2011b); Kamaldar, Mahjoob, Yazdi, Vahid-Alizadeh & Ahmadizadeh (2011a), eliminating the need for explicit knowledge of the underlying physical equations governing the system. However, system identification has its limitations, such as the requirement for high-quality data, the potential for modeling errors if the data is unrepresentative, and the need for careful experimental design.

In Azizi & Keighobadi (2014), the Kane method was utilized to obtain the dynamic model of a spherical robot. Although this method may be more complex to implement compared to simpler approaches like the Newton-Euler method, it offers significant advantages in terms of precision and representation, particularly for complex mechanical systems or detailed analyses. In Sandino, Bejar & Ollero (2013) a comparison of the different methods for modeling a Small-size Helicopter has been done. The results showed that Kane's method offers unique advantages compared to traditional approaches. It incorporates constraints using generalized coordinates and speeds, resulting in concise equations. Constraint forces are considered from the start, and the method is known for its computational efficiency. However, implementing Kane's method necessitates a solid understanding of multibody system dynamics.

2.5.2 Control strategies

A total of 33 control strategies were identified in this study, with sliding mode-based control, PID, PD, fuzzy control, and feedback linearization being the most prevalent. However, these strategies are often enhanced through the incorporation of additional methods, such as fuzzy

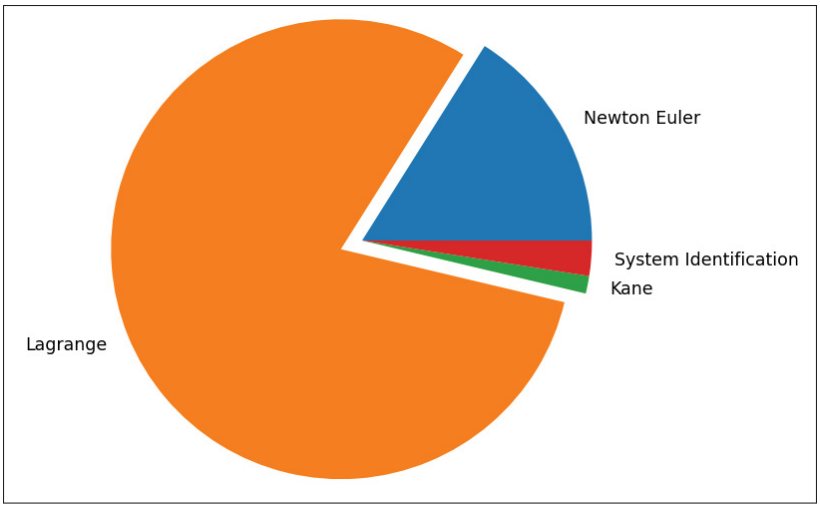

Figure 2.9 Dynamic modeling methods found in SRR papers from 1996 to 2023. The Euler-Lagrange method largely predominates the others.

control or neural network algorithms, into traditional control approaches. Other strategies, such as PD, feedback linearization, and backstepping, are also reported.

This section provides a comprehensive listing and detailed explanation of the various control strategies. Some strategies combine two or three control methods, while other papers independently investigate multiple control strategies for the purpose of comparison. Figure 2.10 provides a summary of the different control strategies documented in the papers.

Among the designs used, the barycentric spherical robot design was the most commonly employed, with sliding mode-based control being the preferred control strategy. However, no direct correlation between the design of the spherical robot and the chosen control strategy was observed.

For an overview of the diverse control strategies included in this study, please refer to Fig. 2.11.

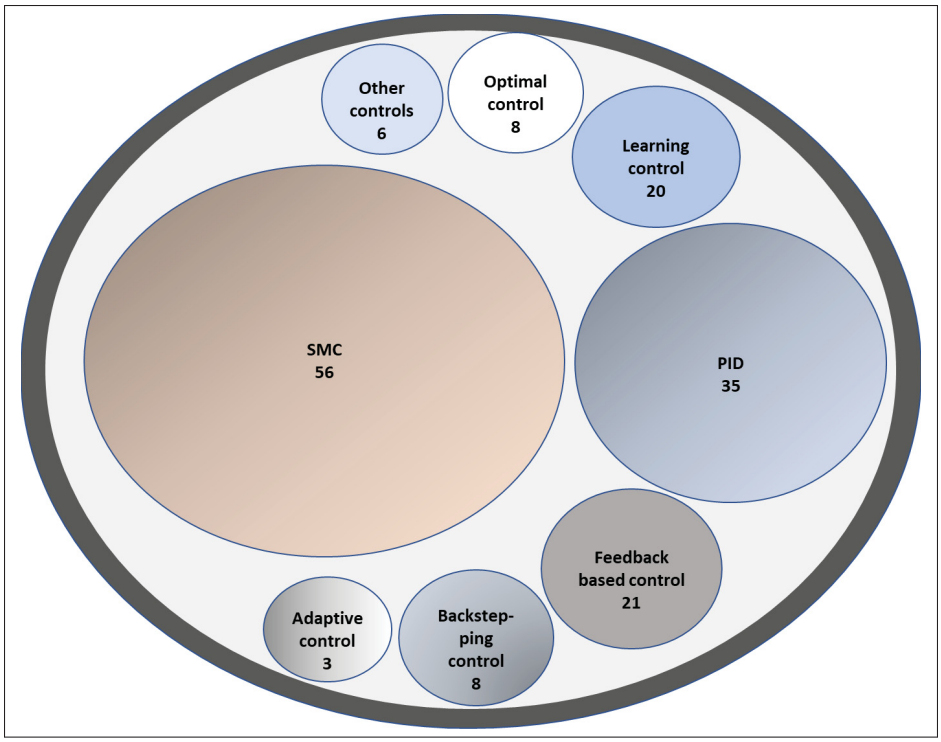

Figure 2.10 Most prominent identified control strategies and their relative importance from the number of related publications ; 'others control' are detailed in Fig. 2.11.

2.5.2.1 Sliding mode control

Sliding mode control is a widely employed technique for controlling various types of robotic systems, including spherical robots and manipulators. Its effectiveness in handling uncertainties and unmodeled disturbances, along with its robust performance, has made it a popular choice. Numerous studies have proposed different SMC-based control strategies, such as cascade sliding mode control (CSMC) Huang, Lin, Lin, Lee & Hwang (2012), high-order sliding mode control (HSMC) Chowdhury, Soh, Foong & Wood (2018a), and adaptive hierarchical sliding mode control (AHSMC) Yue *et al.* (2014a), to enhance the robustness and stability of spherical robots. Researchers have also explored the combination of SMC with adaptive control laws, neural networks, and fuzzy control to address uncertainties and reduce chattering. These hybrid approaches have demonstrated improved tracking accuracy, convergence speed, and robustness

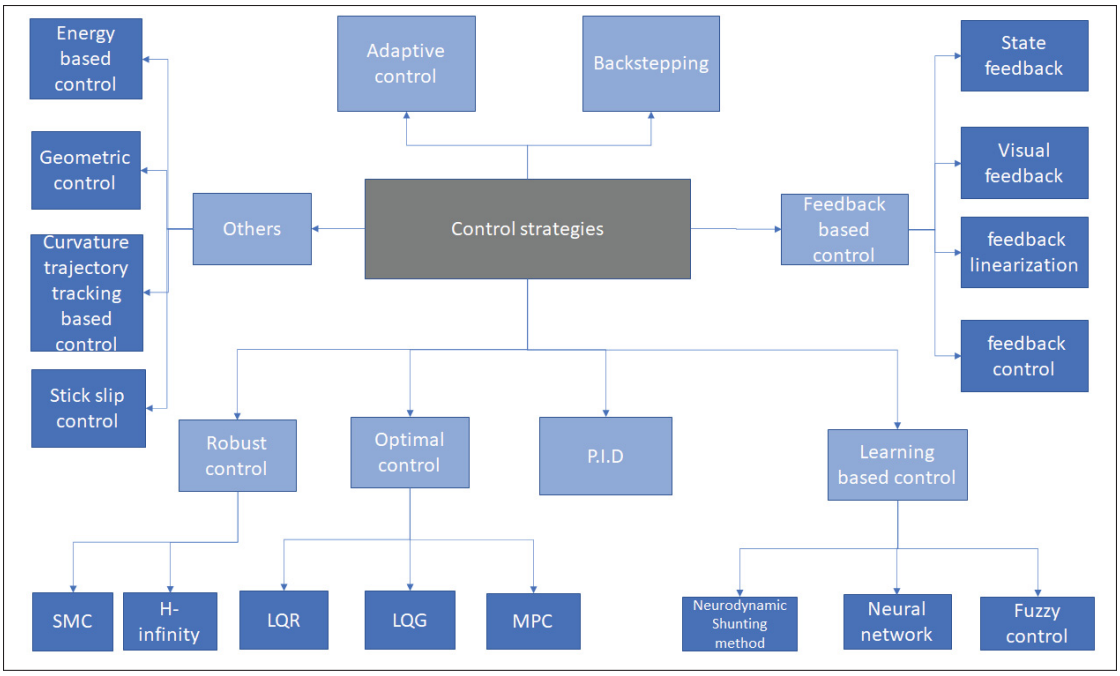

Figure 2.11 Different control strategies included in the study

compared to traditional SMC. Fuzzy control, in particular, is well-suited for complex robotic systems with challenging modeling requirements.

The selection of SMC in the included papers can be attributed to several reasons, primarily the desire to achieve enhanced robustness and cope with uncertainties and unmodeled disturbances. This rationale is discussed in Liu, Sun, Jia & IEEE (2008); Liu & Sun (2010); Wang *et al.* (2011); Zheng, Zhan, Liu & Cai (2011); Yu, Sun, Jia & Zhao (2013); Azizi & Keighobadi (2014); Zhao & Yu (2014); Ayati & Zarei (2017); Li (2020); Nguyen *et al.* (2017).

One promising implementation strategy involves decomposing a complex robotic system into simpler subsystems, where a combination of the dynamic model states and sliding surfaces, known as cascade sliding mode control (CSMC), can be applied as demonstrated in Huang *et al.* (2012). However, conventional CSMC faced challenges in achieving the desired position control performance due to switching constants. To overcome this, the authors introduced positive constants and referred to this modified control method as CSMC1.

Typically, the dynamic model of robots is necessary for designing a sliding mode controller. However, in Li & Zhan (2018), the authors introduced a kinematic-based SMC that can simultaneously track the position and attitude states of a spherical robot. To reduce chattering, a saturation function was added to the traditional SMC approach.

In the pursuit of stability in robot control, Chowdhury *et al.* (2018a) proposed both first and second-order SMC methods. They demonstrated that high-order sliding mode control (HSMC) outperformed the first-order approach, a finding corroborated in Bastola & Zargarzadeh (2019). The control strategy presented in the latter paper reduced chattering and enhanced robust operation in the presence of disturbances.

For improved performance in the face of uncertainties, in Ma, Sun & Song (2020) the authors introduced a fractional-order adaptive integral hierarchical sliding mode control. This approach combines adaptive control laws, hierarchical sliding mode control, and an integrator in the control loop. Comparative analysis with adaptive hierarchical sliding mode control and HSMC revealed that the proposed method exhibited superior convergence speed, stability, and robustness. Adaptive hierarchical sliding mode control was initially proposed in Yue & Liu (2012) and Zhang, Ren & Guo (2021), while HSMC was presented by authors such as Cai, Zhan & Xi (2012) and Chiu, Wang & Hwang (2012).

In Salemizadeh *et al.* (2021), the authors introduced a hybrid super-twisting fractional-order terminal sliding mode control for a rolling spherical robot, which demonstrated higher accuracy and reduced chattering compared to traditional SMC and other SMC-based controls. Hybrid super-twisting fractional-order terminal sliding mode control is an advanced control technique that combines super-twisting control, fractional-order control, and terminal sliding mode control. It aims to achieve robust and accurate control of dynamic systems, especially nonlinear and uncertain systems.

To stabilize a spherical robot moving on an inclined plane, in Roozegar, Ayati & Mahjoob (2017) the authors presented a terminal sliding mode control. They showed that this control approach

effectively reduced chattering compared to SMC and facilitated rapid convergence of the tracking error to zero in less than one second, outperforming SMC for their specific spherical robot.

Some authors have integrated adaptive laws with SMC to enhance results. Adaptive control enables the modeling of uncertainties, thereby reducing chattering Chowdhury, Soh, Foong, Wood & IEEE (2018c). In Sadeghian, Bayani & Masouleh (2015), an adaptive method was employed to identify the exact model. Similarly, in Yue, Liu, Wei & Hu (2014b) the authors employed the same approach to improve robustness and suppress vibrations in the inner suspension platform of a spherical robot. Hierarchical sliding mode control with adaptive methods, referred to as adaptive hierarchical sliding mode control (AHSMC), not only offers improved robustness and parameter insensitivity characteristics but also estimates dynamic disturbances Yue *et al.* (2014a). In Zhang *et al.* (2021), AHSMC was utilized for estimating the moment and rolling friction of a spherical robot.

Authors of Chen *et al.* (2020) combined SMC with neural networks to achieve better performance. The former proposed a radius-based function for controlling the forward movement of the robot, demonstrating good convergence. The latter employed recurrent neural networks in conjunction with SMC (RNNSMC) for stabilization and tracking control. This approach improved the accuracy and performance of the model, with comparisons against fuzzy PID indicating its effectiveness in reducing chattering. Fuzzy PID was chosen as a baseline due to the performance improvements offered by neural network-based control and the suitability of fuzzy control for complex robot modeling.

We note from the above studies that SMC alone often falls short in adequately addressing uncertainties and modeling errors in SRR systems. To tackle this limitation, researchers have also explored the integration of neural networks and fuzzy control with SMC to achieve improved robustness and faster convergence. For instance, in Kayacan, Kayacan, Ramon & Saeys (2013), the authors incorporated neural networks and fuzzy control into the SMC framework, yielding higher robustness and faster convergence in the presence of uncertainties. Similarly, in Andani *et al.* (2018), fuzzy control was combined with SMC to effectively handle parameter

uncertainties. This integration of fuzzy control with SMC proved instrumental in enhancing the overall performance of SRR systems.

2.5.2.2 PID, PI, and PD control strategies

PID control is widely employed by researchers in their studies, either in its traditional form or in combination with other control laws such as fuzzy control, neural networks, Cerebellar-model articulation control, or geometric and adaptive laws. It is probably the most intuitive and less demanding, in terms of processing power, controller for its performance. It is thus common to select this strategy for a fast deployment. For instance, the traditional PID control is utilized in Jayoung, Hyokjo & Jihong (2009) to demonstrate its functionalities. In the work by Roozegar & Mahjoob (2017), PID control is proposed, following Ziegler-Nichols rules, to stabilize a spherical robot on an inclined plane. The Ziegler-Nichols rules are a set of heuristic guidelines used in control theory to tune the parameters of a proportional-integral-derivative (PID) controller. The Authors in Li (2020) apply PID control for pitch angle control. Furthermore, in Cai, Zhan & Xi (2011), PID control is combined with neural networks to compensate for actuators' nonlinearity when single input multiple output PID control fails. This integrated approach exhibits fast convergence and proves to be an efficient method for controlling SRRs.

The application of fuzzy PID control is proposed in Roozegar & Mahjoob (2017) for the motion of a spherical robot, while a comparison with PID control in Sadeghian & Masouleh (2016) demonstrates that fuzzy PID control outperforms PID in terms of performance and stabilization time. In Kayacan, Kayacan, Ramon & Saeys (2012b), fuzzy PID control is combined with feedback linearization and a grey predictor, with the output of the grey predictor utilized instead of the current system outputs. This method exhibits superior performance compared to PID and fuzzy PID controls in terms of overshoot and settling time. Moreover, some studies employ the proportional-integral (PI) control strategy. For example, Belskii & Serykh (2021) proposes PI control for controlling the angular velocity of a spherical robot, and Tang *et al.* (2021) employs PI control for velocity control of a two-wheel differential spherical robot. In Zhang, Jia, Sun,

Gong & IEEE (2009), PI control is employed for real-time control of a spherical robot, with the addition of a genetic algorithm to enhance stability.

PD control is also utilized in certain papers, such as Hanxu, Yili & Qingxuan (2010) and Jia *et al.* (2009), where it is proposed for velocity control of an omnidirectional robot with flywheels. In Nguyen *et al.* (2017) and Niu *et al.* (2014), PD control is employed for controlling the yaw orientation of the spherical robot, while no other strategies are presented for controlling the remaining degrees of freedom.

2.5.2.3 Other control strategies

In addition to sliding mode control (SMC) and proportional-integral-derivative (PID) control, various other control strategies have been employed to control robotic systems. For instance, backstepping control combined with neural networks was used in Ghommam, Mahmoud & Saad (2013) to achieve high-performance cooperative control of a group of mobile robots. The linear quadratic regulator (LQR), dynamic programming, and model predictive control have also been utilized to control spherical robots in some of the included papers. For example, LQR has been used to control robots or stabilize motion, as in Zadeh, Moallem, Asiri & Zadeh (2014), while dynamic programming has enabled optimal motion planning and control of spherical robots in Roozegar, Mahjoob & Jahromi (2016). Feedback linearization has been proposed in Kayacan, Bayraktaroglu & Saeys (2012a); Huang, Zhu, Wang, Huang & Inc (2017) to achieve control and stabilization objectives, and in Hanxu *et al.* (2010), the linear quadratic regulator is used in combination with percentage derivative control for better performance. Some control methods have been used only once, such as the active disturbance rejection control in Zhou *et al.* (2021) to achieve trajectory tracking control for biomimetic spherical robots without model parameter information, energy-based control in Sun (2021) for a spherical robot to track high moving speeds, and H-infinity control in Rigatos *et al.* (2019) to provide a solution to the robot's optimal control problem under model uncertainty and external perturbation.

2.6 Experiments and sensing

2.6.1 Simulations vs experimental validation

In all included papers, authors performed either experiments or simulations in order to validate or verify the feasibility of the proposed control strategies. From the control aspect, 32 % of the papers performed experiments to validate their control strategies while 78 % realized only simulations. These validations were done in numerical simulation software such as Matlab Simulink Cai *et al.* (2012) or by implementing the control strategy on a prototype Jia *et al.* (2009). If we look only at BSRs, the broad mechanism category with the largest number of publications over the years, a significant portion of them included a physical prototype, namely 50 % for pendulum-based BSRs, 38 % with sliding masses and 82 % for IDU-driven BSRs. These numbers are not unexpected, as robots with an IDU are generally cheaper to prototype. On the opposite end, using sliding masses increases the mechanical complexity of the system, as well as requiring more complex control schemes, the sliding masses needing to continuously change direction to provide a uniform and continuous motion of the sphere.

Beyond the presentation of a prototype, experimental validation with different tests and scenarios is less common. For instance, Chowdhury et al. Chowdhury *et al.* (2018b) conducted experiments in both indoor (smooth surface) and outdoor environments (rough surfaces) to validate their model and their control strategy as well. In the paper by Alves and Dias Alves & Dias (2003), a path curvature-based control was presented. Some authors used motion capture systems able to track markers inside the shell in order to validate the accuracy of robot localization Ajay *et al.* (2015). When conducting experiments, different metrics were selected for the validation of the results. The most common were the overshoot, the steady state response, the rise time, the convergence time, and the maximum absolute value of motion trajectory error.

2.6.2 Embedded sensing

The few reviewed papers that progressed to prototype validation necessitated the incorporation of sensing components to close the control loop. The majority of these papers employed commonly used sensors, including accelerometers, cameras, and encoders. Accelerometers, typically housed within an inertial measurement unit (IMU), were utilized in some papers to acquire feedback on the robot's state. Notably, Alves & Dias (2003) proposed to use a three-axis accelerometer combined with a three-axis rate gyroscope to obtain information about the robot's acceleration, angular velocity, and position. In Zhao *et al.* (2010), the feedback is obtained from a module of sensors that consists of encoders of the servomotors, angular rate sensors, angular acceleration sensors, and directional gyro, which are all microelectromechanical systems (MEMS) devices However, IMUs were predominantly deployed to provide orientation information in studies such as Alves & Dias (2003); Niu *et al.* (2014); Zhai *et al.* (2015); Zhang, Ren & Zheng (2022, 2023); Zheng *et al.* (2021). To mitigate noise and drift issues, an extended Kalman filter was applied to the IMUs in Liu *et al.* (2022).

Some researchers incorporated additional sensors into their systems. Encoders were commonly used in conjunction with IMUs Liu, Sun & Jia (2009); Urakubo, Monno, Maekawa & Tamaki (2016); Urakubo, Osawa, Tamaki, Tada & Maekawa (2012); Ajay *et al.* (2015); Chowdhury, Vibhute, Soh, Foong & Wood (2017); Hu *et al.* (2022); Ling *et al.* (2022); Roy Chowdhury, Soh, Foong & Wood (2017); Wang *et al.* (2021, 2023), while cameras were employed for real-time position tracking in Zhang & Ren (2022); Zhang *et al.* (2021). In Hanxu *et al.* (2010), an IMU, gyroscope, and inclinometer were combined to acquire the pitch, roll, and yaw angles, as well as the lean angles and spin rate of the robot. To improve the accuracy of position measurement considering slipping, Cai *et al.* (2012) proposed a vision system in addition to an IMU. Vision systems were utilized by other authors for obtaining feedback information as well. For example, Jaimez, Castillo, García & Cabrera (2012) proposed a system comprising four infrared cameras along with dedicated software to determine the position of the robot in space. In Roozegar, Mahjoob & Ayati (2018), an RGB camera is used to track the spherical robot pose at 30Hz (each frame). Similarly, in Roozegar *et al.* (2016); Sakalli, Beke & Kumbasar (2018), a camera system

was utilized to acquire the robot's position. Furthermore, in Belzile & St-Onge (2022a), the combination of a depth camera and a LIDAR was used to map the environment and infer the robot's position in the map (Simultaneous Localization and Mapping - SLAM). It should be noted that employing camera systems either requires a transparent shell or a turret to house the camera, resembling the popular design of BB-8.

An overview of the sensors used in the reviewed papers is depicted in Fig. 2.12.

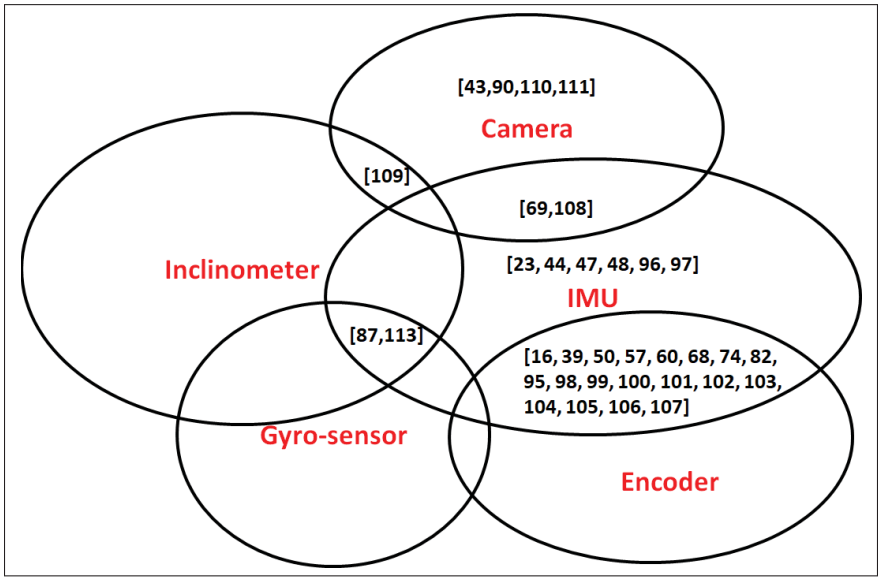

Figure 2.12 Embedded sensors distribution and combination in the publications covered. The vast majority combine IMUs with encoders

2.7 Discussion

After a comprehensive analysis of the papers, several challenges associated with spherical robots have been identified. While some of these challenges have been addressed in the literature, others remain unexplored. In this section, we will delve into these challenges and discuss potential avenues for further research.

One significant challenge arises from the limited number of contact points that spherical robots have with the ground. This constraint makes it challenging to employ traditional sensors similar

to those used in wheeled or legged robots for measuring motion and orientation. Although some papers suggest using IMUs for measurements, controlling the robot becomes problematic due to drift errors inherent in IMUs. Consequently, there is a research opportunity to explore robust control methods that can effectively model disturbances and uncertainties. However, relying solely on proprioceptive measurements may prove insufficient for most realistic missions such as exploration and inspection.

To overcome the limitations of proprioceptive measurements, additional sensors like cameras, LIDAR, or ultrasonic sensors can be integrated to complement IMU data and provide more accurate information about the robot's surroundings and motion. An example of such integration can be found in Belzile & St-Onge (2022a), where a camera and a LIDAR are utilized. However, the use of cameras and LIDARs in spherical robots introduces challenges related to refraction and distortion. These phenomena can alter distance and position measurements captured by the sensors, leading to perceptual errors. Moreover, inadequate perception of the environment's geometry can result in errors in motion planning and localization. Thus, investigating the impact of refraction and distortion becomes crucial in enhancing perception precision, motion planning, localization, and sensor calibration. Such research efforts would ultimately improve the reliability and efficiency of navigation for robots equipped with cameras and LIDARs.

When considering the integration of cameras and LIDARs, it is imperative to ensure a clear line of sight. Alternatively, cameras can be positioned outside the shell on both sides, as demonstrated in Kolbari, Ahmadi, Bahrami, Janati & Ardekany (2018). However, integrating cameras outside a non-transparent shell may impose limitations on the robot's omnidirectional movements and increase the risk of camera damage.

The unique shape and locomotion mechanism of spherical robots pose significant challenges in obstacle avoidance. These robots rely on changing their center of gravity or rolling in different directions to move. However, the lack of independent directional control makes efficient navigation around obstacles challenging. Additionally, SRRs maintain contact with the ground or surfaces using a single point or a limited set of points, which can affect their stability and

maneuverability, especially when encountering uneven terrain or obstacles with varying heights. Maintaining balance and stability while avoiding obstacles becomes increasingly challenging in such scenarios. One potential solution to address this challenge is incorporating jumping mechanisms in spherical robots, enabling them to overcome obstacles vertically. By introducing a jumping mechanism, spherical robots gain the ability to leap over barriers, gaps, or rough terrain that would otherwise be challenging or impossible to traverse with rolling or sliding locomotion alone. However, achieving controlled leaps while managing the position of the center of mass and the point of application of the propulsion force remains an open challenge due to the mechanical complexity involved.

Moreover, two distinct approaches can be employed to tackle the intricate dynamics of spherical robots : the decoupled approach and the complete approach. The decoupled dynamic approach involves separating the transversal and longitudinal motions of the robot and studying them independently. This approach simplifies the dynamics and reduces computational effort. On the other hand, the complete dynamic approach involves modeling the robot without decoupling the motions, which adds complexity to the system. Comparing these two approaches can be valuable in understanding their respective advantages and drawbacks, enabling individuals to determine the most suitable approach for their needs.

In addition to the aforementioned challenges, controlling a spherical robot can be particularly demanding, especially for non-holonomic systems such as pendulum-driven spherical robots. These non-holonomic systems possess motion constraints that cannot be easily integrated into their configuration space. As a result, designing control laws capable of steering the system along a desired trajectory becomes difficult. Unlike holonomic systems, non-holonomic systems require careful consideration of their constraints and dynamics to develop control laws that can achieve the desired motion. Therefore, further research is needed to explore effective control strategies tailored to non-holonomic spherical robots.

2.8 Conclusion

The paper provides a comprehensive analysis of spherical robots, covering various aspects such as design, locomotion, control, and embedded sensing. It reviews multiple research papers to gain insights into the state of the art in spherical robot development. The design of spherical robots involves considerations such as the mechanisms for locomotion. Different locomotion mechanisms are discussed, including pendulum-driven systems, internal mass shifting, COAMs, and shell transformation. The paper explores various control strategies for spherical robots, with a focus on efficiency, stability, robustness, and feasibility. A comprehensive analysis identified a total of 33 control strategies used for controlling spherical robots. Among these strategies, the findings indicate that sliding mode-based control is the most prevalent approach employed in the control of spherical robots. The challenges associated with spherical robots encompass the limitations posed by their contact points, the integration of additional sensors, obstacle avoidance, controlled leaps, and control of non-holonomic systems. Addressing these challenges through targeted research efforts would drive advancements in spherical robotics, paving the way for more capable and versatile robotic systems in various applications.

This review emphasizes the importance of ongoing research and innovation in spherical robot design, locomotion, control, and embedded sensing. It emphasizes the potential of spherical robots in various applications and identifies areas for future exploration, such as refining control strategies, addressing challenges in obstacle avoidance, and comparing different approaches to modeling their dynamics.

Overall, the paper provides a comprehensive overview of spherical robot research, highlighting the current state of the field, key challenges, and potential avenues for further advancement.

Acknowledgment

This work was supported by the NSERC Discovery Grant (RGPIN-2020-06121). We would like to express our gratitude to Simon Bonnaud for his valuable support for the redaction of this manuscript.

CHAPITRE 3

MODELING AND CONTROL OF A PENDULUM-DRIVEN SPHERICAL ROBOT USING SLIDING MODE CONTROL

Aminata Diouf[1] , David St-Onge[1] , Maarouf Saad[2]

[1] Department of Mechanical Engineering,École de technologie supérieure,
1100 Notre-Dame Ouest, Montréal, Québec, Canada H3C 1K3
[2] Department of Electrical Engineering,École de technologie supérieure,
1100 Notre-Dame Ouest, Montréal, Québec, Canada H3C 1K3

Article submitted in the journal "Dynamic Systems, Measurement, and Control " in October 2023.

3.1 Abstract

This paper presents modeling and control strategies for ARIES, a pendulum-driven spherical robot designed for space exploration. The intricate dynamics of spherical rolling robots present challenges in both modeling and control, owing to their nonlinearity and non-holonomic characteristics. Furthermore, ARIES features an internal pendulum actuated by a cylindrical drive, a mechanism that has not been previously addressed in the modeling and control of spherical robots. We conduct a comparative analysis of three dynamic models : decoupled (4 states), reduced (5 states), and complete (7 states), evaluating their accuracy and efficiency when integrated with a model-based control strategy. Various control strategies, such as sliding mode control (SMC) and computed torque control, are assessed. This study offers comprehensive guidelines for achieving effective trajectory tracking. The simulation results underscore the strengths and limitations of each approach.

3.2 Introduction

Spherical rolling robots (SRRs) have gained significant attention in recent years and are being utilized in various applications, including space, underwater, and extreme environment exploration, replacing the traditional use of rovers. They provide significant advantages for space exploration. They can move in any direction, offering agility in planetary terrains. They are

less likely to get stuck, even in soft soils or on steep slopes, due to their continuous orientation adjustment. Spherical robots have a simple design with fewer moving parts, enhancing reliability and reducing maintenance needs. Their compact size is efficient for storage and launch on spacecraft and it allows them to access tight spaces in planetary environments making them versatile for various space missions. Notable examples of SRRs include the NASA Beach ball, employed in space exploration [3], and Rollo, the first spherical robot developed at Helsinki University, used for exploring hostile environments Halme *et al.* (1996).

An in-depth analysis of rolling in robotics is presented in a research paper Armour & Vincent (2006b), which explores the historical designs of Spherical Rolling Robots (SRRs). Meanwhile, another review Chase & Pandya (2012) is primarily centered on the various actuation mechanisms that are unique to spherical robots.

There are three main designs for spherical robots : barycentric spherical robots (BSRs), conservation of angular momentum (COAM) spherical robots, and shell transformations. BSRs, the most common design, rely on shifting the center of mass (COM) of the inner mechanism to achieve rolling. This category includes pendulum-driven spherical robots Balandin, Komarov & Osipov (2013); Liu *et al.* (2009); Kayacan *et al.* (2012a), which utilize a pendulum as the inner mechanism for COM shifting, internal drive unit (IDU) spherical robots Ghanbari, Mahboubi & Fakhrabadi (2010); Nakashima, Maruo, Nagai & Sakamoto (2018), where a wheeled robot is placed inside the spherical shell for locomotion, and sliding mass spherical robots Bowkett *et al.* (2017), which use sliding masses to control the robot's position.

Modeling spherical robots poses substantial challenges because of their intricate dynamics including conservation of angular momentum, gravity effects, and the rolling contact. The complex dynamics arise from their ability to move in any direction, the need to account for the changing distribution of mass as they roll, and the intricate balance between various forces acting on them during locomotion. The complexity of controlling spherical robots directly follows from the challenges of their dynamics modeling, inherently nonlinear and non-holonomic. A

[3] https://ntrs.nasa.gov/citations/19950070425

multitude of control strategies are described in the literature. Researchers have proposed a range of innovative techniques and methods to tackle these control challenges, each with its own set of advantages and trade-offs. These efforts underline the significance of addressing the complexities associated with controlling spherical robots and finding effective solutions to harness their potential in various applications.

A comprehensive review of different control strategies in the literature can be found in Diouf, Belzile, Saad & St-Onge (2023). This review encompasses a range of control strategies, including sliding mode control (SMC) and proportional-integral-derivative (PID) control. The review concludes that few studies have conducted experiments to validate and compare these control strategies with existing methods and that the majority of these studies simplify their dynamic model (linearisation or decoupled dynamics) without proper assessment of the impacts on the performance.

For non-holonomic systems such as pendulum-driven spherical robots, the control can be particularly demanding. These non-holonomic systems possess motion constraints that cannot be easily integrated into their configuration space. As a result, designing control laws capable of steering the system along a desired trajectory becomes difficult. Unlike holonomic systems, non-holonomic systems require careful consideration of their constraints and dynamics to develop control laws that can achieve the desired motion.

This paper focuses on the modeling and the control of ARIES short for "Autonomous Robotic Intelligent Explorer Sphere," Belzile & St-Onge (2022b), a pendulum-driven spherical robot designed specifically for space exploration. ARIES employs a unique propulsion system and is characterized by a spherical shell that houses a cylindrical actuated mechanism, which operates similarly to a pendulum. This mechanism is thoroughly detailed in the reference Belzile & St-Onge (2022a). The cylindrical actuated joints of ARIES are mechanical components with two degrees of freedom, facilitating both rotational and translational movement along a shared axis. To accomplish this goal, we employed three distinct dynamics approaches : decoupled, complete, and reduced dynamics, for the purpose of conducting a comparative analysis. Furthermore, we

compared ARIES' cylindrical drive design with an alternative double pendulum design, which represents a more common design choice within the literature. Additionally, we evaluated the control strategies applied to ARIES, specifically comparing the utilization of sliding mode control with computed torque control.

The paper is organized as follows : Section 2 presents the related work, Section 3 presents the dynamic modeling of ARIES, Section 4 addresses trajectory tracking and control, Section 5 presents simulation results, and Section 6 discusses the hardware implementation that is planned to be done in the next study. The prototype of ARIES is depicted in Figure 3.1.

To the best of our knowledge, the original contributions of this paper are :

1. Extension of Dynamic Modeling with Resolution and Lagrange Multipliers Handling : This article builds upon the groundwork laid in Belzile & St-Onge (2022a) and Belzile & St-Onge (2022b) by extending the dynamic modeling of ARIES. The focus is on completing the dynamic modeling through the integration of decoupled and complete dynamics. Notably, this extension includes a comprehensive resolution approach and addresses the handling of Lagrange multipliers to enhance the fidelity of the dynamic model.

2. Introduction of Reduced Dynamics : A primary contribution lies in the introduction of a reduced dynamic derived from the complete dynamic. This reduction is achieved by minimizing the number of generalized parameters, ultimately resulting in a dynamic equation without the need for Lagrange multipliers.

3. Implementation of Sliding Mode Controller : An advanced sliding mode controller for ARIES is implemented, utilizing the three distinct dynamic models. This adds a practical dimension to the theoretical advancements, demonstrating the applicability of the proposed models in control systems.

4. Comparative Analysis of Dynamic Models : A significant contribution involves providing a comparative analysis of the three dynamic models. This comparative study enhances the overall

understanding of ARIES dynamics, offering insights into the strengths and limitations of each model.

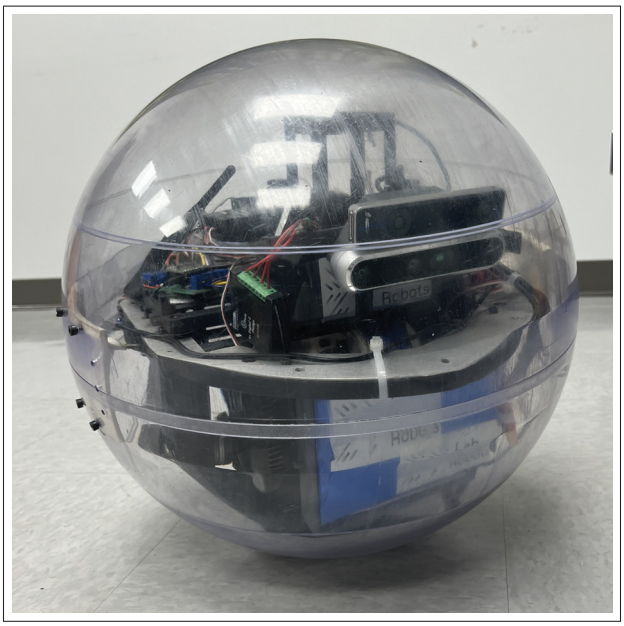

Figure 3.1 Prototype of ARIES

3.3 Related work

In our prior research Diouf *et al.* (2023), we explored a wide array of literature to uncover various methodologies for modeling and controlling spherical robots. The unique motion characteristics of these robots introduce intricate considerations for both kinematic and dynamic modeling. While some studies, such as those by Nam *et al.* (2019); Li & Zhan (2019), focus exclusively on kinematic models, the majority prefer dynamic models due to factors like the impact of conservative forces, as seen in the pendulum gravity effect. However, when applicable, the kinematic-only approach offers a simplified perspective on system behavior, emphasizing motion and positioning rather than complex dynamics.

Among the techniques used to derive dynamic models, the Euler-Lagrange method is commonly employed across various papers. This systematic approach, grounded in energy principles, is invaluable for modeling mechanical systems. Nevertheless, incorporating motion constraints can

involve the use of Lagrange's multipliers, which introduces computational complexities related to constraint force calculation.

In contrast, the Newton-Euler method, a fundamental tool in robotics, physics, and control systems, provides explicit equations of motion and recursive formulations, making it easier to analyze complex mechanical systems. Its breakdown of inter-body forces simplifies the examination of system components. On the other hand, system identification methods focus on mathematical models based on input-output relationships, departing from physics-based representations. As demonstrated in studies like Kamaldar *et al.* (2011b,a), this approach bypasses the need for a deep understanding of underlying physical equations but requires high-quality data and careful experimental design to mitigate potential modeling errors.

In the realm of dynamic modeling, Azizi & Keighobadi (2014) applied the Kane method to develop a dynamic model for spherical robots. Although more complex to implement compared to simpler approaches like Newton-Euler, this method offers precision and representational advantages, particularly for intricate mechanical systems. Similarly, Sandino *et al.* (2013) compared various modeling methods for a Small-size Helicopter, highlighting the distinct benefits of Kane's method. This technique, which utilizes generalized coordinates and speeds to account for constraints, yields concise equations but demands a strong grasp of multibody system dynamics.

Transitioning to the field of control strategies, we encounter a diverse landscape where various techniques interact, often augmented by additional methods such as fuzzy control or neural network algorithms integrated into conventional control approaches. Other strategies, including PD control, feedback linearization, and backstepping, have also been explored.

At the forefront of control strategies stands sliding mode control (SMC), emerging as a widely adopted technique for various robotic systems, including spherical robots. Known for its robustness against uncertainties and unmodeled disturbances, SMC has been the focus of numerous studies. Notable variations of SMC, such as cascade sliding mode control (CSMC) Huang *et al.* (2012), high-order sliding mode control (HSMC) Chowdhury *et al.* (2018a), and

adaptive hierarchical sliding mode control (AHSMC) have been proposed to enhance robustness and stability. Combining SMC with adaptive control, neural networks, and fuzzy control has led to improvements in tracking accuracy, convergence, and overall robustness compared to traditional SMC.

Meanwhile, PID control remains a popular strategy for controlling spherical robots. Whether used on its own or in combination with fuzzy control, neural networks, or other methods, PID control offers an intuitive and computationally efficient choice for rapid implementation. Examples include traditional PID control Jayoung *et al.* (2009), PID for stabilization Roozegar & Mahjoob (2017), and PID for pitch angle control Li (2020). Similarly, proportional-integral (PI) control, as in Belskii & Serykh (2021), and proportional-derivative (PD) control, as exemplified by Hanxu *et al.* (2010), find applications in velocity and yaw control, respectively. Furthermore, combining PID control with neural networks is used to address actuator nonlinearity Cai *et al.* (2011).

Beyond SMC and PID, the landscape of control strategies broadens with the incorporation of various approaches. Linear quadratic regulator (LQR), dynamic programming, and model predictive control take center stage for optimal motion and control in Zadeh *et al.* (2014) and Roozegar *et al.* (2016). Feedback linearization emerges as a suitable choice for control in works such as Kayacan *et al.* (2012b) and Huang *et al.* (2017). Genetic algorithms, meanwhile, enhance the stability of PI control in Zhang *et al.* (2009). Notably, unique strategies like active disturbance rejection control, energy-based control Sun (2021), and H-infinity control Rigatos *et al.* (2019) address specific challenges, further enriching the array of control methodologies.

These previous studies served as inspiration for implementing sliding mode control to manage ARIES. However, it's essential to acknowledge certain limitations in these studies. Firstly, a majority of them primarily remained theoretical in nature, lacking experimental validation for their dynamic models and control strategies. Additionally, many of these papers validated their control strategies without conducting comparative assessments against alternative approaches. Furthermore, most of these studies exclusively utilized decoupled dynamics, without exploring other methods of modeling spherical robots and assessing the performance of each approach. In

our paper, we address these limitations by validating our dynamic models through open-loop experiments. Furthermore, we perform a performance analysis to evaluate the effectiveness of each dynamic model. Additionally, we compare our chosen sliding mode control (SMC) with computed torque control to validate our selection.

3.4 Dynamic modeling and transformation

ARIES is a barycentric spherical robot with two degrees of freedom (DOFs). It features an actuated cylindrical joint that acts as a pendulum. The robot's motion on the ground is achieved by displacing the center of mass through the actuated pendulum. In order to enable steering capabilities and not just forward and backward rolling in a single direction, two controlled DOFs are necessary. The cylindrical joint allows for translation u and rotation α within the sphere. We define F_s as the frame fixed to the center of mass (COM) of the sphere, F as the inertial frame, and F_p as the frame fixed to the COM of the pendulum. A reference frame F_m is attached to the center of the sphere. This frame undergoes a translation with respect to a reference frame F_0 that makes an angle ψ with the principal frame. ψ corresponds to the direction of the robot. These frames are represented in Fig. 3.2. Some elements of this section are repeated from Belzile & St-Onge (2022b) and Belzile & St-Onge (2022a) for readability since our derivation presents several differences to stress the coherence between the models and reach the reduced state not presented earlier.

The physical parameters of the robot are listed in Tab 3.1.

3.4.1 Decoupled Dynamics

To simplify the nonlinear dynamics of the system, a decoupled approach can be used initially, as detailed in Kayacan *et al.* (2012a) for the double pendulum or in Belzile & St-Onge (2022a) for ARIES. This approach involves separating the velocities corresponding to the front rolling and the orientation of the sphere. It is a conceptual approach often used in the literature. Additionally, the angular velocity around z-axis $\dot{\psi}$ will be assumed negligible compared to the other angular

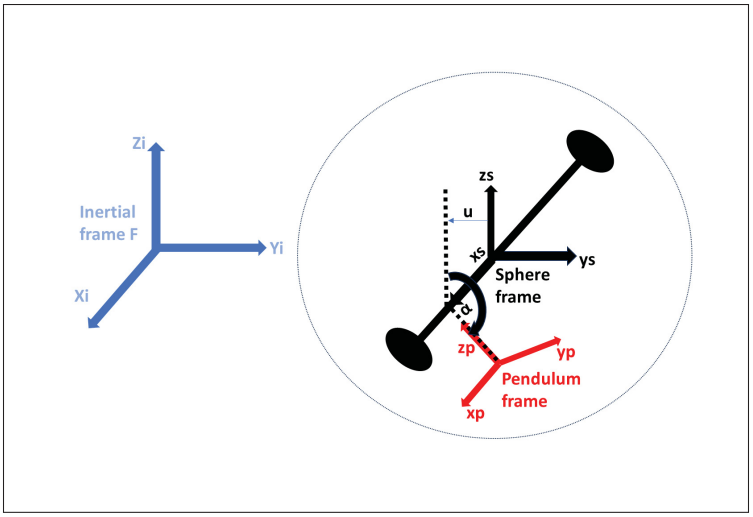

Figure 3.2 Frames for modeling

Tableau 3.1 Physical Parameters

Parameter	**Description**
R	Radius of the sphere
r	Distance between the center of the sphere and COM of the pendulum
m_s	Mass of the shell
m_p	Mass of the pendulum
I_s	Moment of inertia of the shell ($I_s = \frac{2\,R^2\,m_s}{3}$)
I_p	Moment of inertia of the pendulum ($I_p = \frac{m_p\,r^2}{3}$)
θ	Angle of rotation of the sphere following the x-axis of F_0
α	Rotational output of the cylindrical joint
u	Translational output of the cylindrical joint
g	Gravitational acceleration
G	Reduction ratio of the cylindrical joint
p	Pitch of the lead screws

velocities. For the rotational motion, the x-axes of F_m and F_s are assumed to be collinear, and the rotation angle around these axes is θ. For tilting, however, it is the y-axes of F_m and F_s that are collinear, and the corresponding rotation angle is ϕ. The corresponding transformation matrices are defined as follows :

$$\mathbf{R}_x = \begin{bmatrix} 1 & 0 & 0 \\ 0 & \cos\theta & -\sin\theta \\ 0 & \sin\theta & \cos\theta \end{bmatrix} \tag{3.1}$$

$$\mathbf{R}_y = \begin{bmatrix} \cos\phi & 0 & \sin\phi \\ 0 & 1 & 0 \\ -\sin\phi & 0 & \cos\phi \end{bmatrix} \tag{3.2}$$

Velocities and positions for transverse and longitudinal movements will be differentiated by the superscripts "x" and "y" in their expressions. Consequently, linear and angular velocities of the sphere in frame F can be defined as follows :

$$\begin{aligned} {}^{x}V_{sf} &= \begin{bmatrix} 0 & -R\dot{\theta} & 0 \end{bmatrix}^T, \quad {}^{x}\omega_{sf} = \begin{bmatrix} -\dot{\theta} & 0 & 0 \end{bmatrix}^T \\ {}^{y}V_{sf} &= \begin{bmatrix} R\dot{\phi} & 0 & 0 \end{bmatrix}^T, \quad {}^{y}\omega_{sf} = \begin{bmatrix} 0 & -\dot{\phi} & 0 \end{bmatrix}^T \end{aligned} \tag{3.3}$$

Here, θ represents the rotation angle, and ϕ represents the tilting angle. Similarly, the position of the cylindrical joint can be expressed in frame F_s as :

$$\begin{aligned} {}^{x}r_{pf_s} &= \begin{bmatrix} 0 & r\sin\alpha & -r\cos\alpha \end{bmatrix}^T \\ {}^{y}r_{pf_s} &= \begin{bmatrix} k_p u & 0 & -r \end{bmatrix}^T \end{aligned} \tag{3.4}$$

The angular velocity of the pendulum's center of mass along the x-axis of F_s is defined by the following relation :

$${}^{x}\omega_{pf_s} = \begin{bmatrix} \dot{\alpha} & 0 & 0 \end{bmatrix}^T \tag{3.5}$$

The pendulum undergoes a translation u with respect to the x-axis of F_s. Therefore, the angular velocity ${}^{y}\omega_{pf}s$ is zero.

The position of the pendulum's center of mass can also be expressed in frame F using the transformation matrices R_x and R_y :

$$\begin{aligned} {}^{x}r_{pf} &= R_x {}^{x}r_{pf_s} \\ {}^{y}r_{pf} &= R_y {}^{y}r_{pf_s} \end{aligned} \tag{3.6}$$

Consequently, linear and angular velocities of the pendulum's center of mass can be defined in frame F as follows :

$$\begin{aligned} {}^{x}\omega_{pf} &= {}^{x}\omega_{sf} + R_x {}^{x}\omega_{pf_s} \\ {}^{y}\omega_{pf} &= {}^{y}\omega_{sf} \\ {}^{x}V_{pf} &= {}^{x}V_{sf} + {}^{x}\omega_{pf} \times {}^{x}r_{pf} \\ {}^{y}V_{pf} &= {}^{y}V_{sf} + {}^{y}\omega_{pf} \times {}^{y}r_{pf} + V_{sp} \end{aligned} \tag{3.7}$$

Here, V_{sp} is the velocity of the pendulum with respect to the sphere. It is defined as follows :

$$V_{sp} = R_y \begin{bmatrix} \dot{u} \\ 0 \\ 0 \end{bmatrix} \tag{3.8}$$

The Lagrange method will be used to obtain the equations of the decoupled dynamics. The Lagrangians L_x and L_y, corresponding to the rotation and tilting of the robot, will be defined. The rotation is associated with the generalized coordinates $q_1 = [\theta\ \alpha]^T$, while tilting is associated with $q_2 = [\phi\ u]^T$. The kinetic energies E_{cx}, E_{cy}, and the potential energies E_{p_x}, E_{p_y} are defined in the following equations :

$$
\begin{aligned}
{}^{x}E_c &= \frac{1}{2}(m_s\|{}^{x}V_{sf}\|^2 + m_p\|{}^{x}V_{pf}\|^2 + I_s\|{}^{x}\omega_{sf}\|^2 + I_p\|{}^{x}\omega_{pf}\|^2) \\
{}^{y}E_c &= \frac{1}{2}(m_s\|{}^{y}V_{sf}\|^2 + m_p\|{}^{y}V_{pf}\|^2 + I_s\|{}^{y}\omega_{sf}\|^2 + I_p\|{}^{x}\omega_{pf}\|^2) \\
{}^{x}E_p &= m_p g {}^{x}r_{pf_z} \\
{}^{y}E_p &= m_p g {}^{x}r_{pf_z}
\end{aligned}
\tag{3.9}
$$

Here, $\|{}^{x}V_{sf}\|^2$, $\|{}^{x}V_{pf}\|^2$ represent the square of the two-norm of the velocity vector of the center of mass of the sphere and the pendulum, respectively. ${}^{x}r_{pf_z}$ represents the component along the z-axis of the position of the pendulum in the principal frame.

Therefore, the Lagrangians can be defined as :

$$
\begin{aligned}
L_x &= {}^{x}E_c - {}^{x}E_p \\
L_y &= {}^{y}E_c - {}^{y}E_p
\end{aligned}
\tag{3.10}
$$

The Lagrange equations are then :

$$\frac{d}{dt}\left(\frac{\partial L_x}{\partial \dot{\alpha}}\right) - \frac{\partial L_x}{\partial \alpha} = \tau_\alpha \tag{3.11a}$$

$$\frac{d}{dt}\left(\frac{\partial L_x}{\partial \dot{\theta}}\right) - \frac{\partial L_x}{\partial \theta} = \tau_\theta \tag{3.11b}$$

$$\frac{d}{dt}\left(\frac{\partial L_y}{\partial \dot{\phi}}\right) - \frac{\partial L_y}{\partial \phi} = \tau_\phi \tag{3.11c}$$

$$\frac{d}{dt}\left(\frac{\partial L_y}{\partial \dot{u}}\right) - \frac{\partial L_y}{\partial u} = f \tag{3.11d}$$

Here, $\tau_\theta = \tau_\alpha = \tau$ represents the moment at the output of the cylindrical joint, f is the force at the output of the cylindrical joint, and τ_ϕ represents the moment applied to the sphere, defined by $\tau_\phi = 0$ because the axis of the frame passes through the center of the pendulum. Noting $q = [\theta\ \alpha\ \phi\ u]^T$, these four equations can be written in the form :

$$M(q(t))\ddot{q}(t) + V(q(t), \dot{q}(t)) = Q \tag{3.12}$$

With M the mass matrix which is positive definite symmetric This equation can be solved symbolically using 3.13

$$\ddot{q} = M^{-1}(Q - V) \tag{3.13}$$

We can obtain the generalized coordinates by integrating twice $\ddot{q}$.

3.4.2 Complete Dynamics

In this subsection, we consider the complete dynamic model of the system without any simplification. To establish the orientation between the inertial and the sphere frames, we introduce Euler angles and intermediate frames F' and F'' as in Belzile & St-Onge (2022b).

The movement between F_s and F can be described as follows :

- A rotation ψ around the z-axis of F_s resulting in the frame F'.
- A rotation θ around the y-axis of F' resulting in the frame F''.
- A rotation ϕ around the x-axis of F'' resulting in the frame F.

The transformation matrices and the kinematic relations are the same as in Belzile & St-Onge (2022b).

The Lagrange method is used to derive the dynamic equations of the system. To achieve this, kinetic and potential energies, as well as generalized coordinates, are defined. Kinetic energy will be denoted as E_c, potential energy as E_p, and the generalized coordinates will be defined using the matrix **q**. These various parameters are defined in the following equations :

$$\begin{aligned} q &= \begin{bmatrix} \psi & \theta & \phi & x_s & y_s & \alpha & u \end{bmatrix}^T \\ E_c &= \frac{1}{2}\left(m_s\|\dot{r}_s\|^2 + m_p\|\dot{r}_p\|^2 + I_s\|\dot{w}_{s_s}\|^2 + I_p\|\dot{w}_{s_p}\|^2\right) \\ E_p &= m_p g r_{p_z} \end{aligned} \tag{3.14}$$

Here, $\|\dot{r}_s\|^2$ and $\|\dot{r}_p\|^2$ represent, respectively, the norm of the velocity vector of the center of mass of the sphere and the pendulum. r_{p_z} represents the Z-component of the pendulum's position in the principal frame. $\|\dot{w}_{s_s}\|$ and $\|\dot{w}_{s_p}\|$ represent, respectively, the norm of the angular velocity vector of the center of mass of the sphere and the pendulum.

Therefore, the Lagrangian **L** can be defined as :

$$L = E_c - E_p \tag{3.15}$$

There is an additional complexity in the modeling due to the assumption of rolling without slipping, which introduces a constraint on the parameters. In fact, since the robot is assumed to roll without slipping, the velocity of the contact point between the robot and the ground is equal to zero. These constraints can be expressed as follows :

$$\begin{cases} \dot{x}_s - R\left(\dot{\theta}\,\cos(\psi) + \dot{\phi}\,\cos(\theta)\,\sin(\psi)\right) & = 0 \\ \dot{y}_s - R\left(\dot{\theta}\,\sin(\psi) - \dot{\phi}\,\cos(\psi)\,\cos(\theta)\right) & = 0 \end{cases} \tag{3.16}$$

Alternatively, we can express these constraints in matrix form as :

$$A\dot{q} = 0 \tag{3.17}$$

where A is a 2×7 is defined as :

$$\begin{pmatrix} 0 & -R\,\cos(\psi) & -R\,\cos(\theta)\,\sin(\psi) & 1 & 0 & 0 & 0 \\ 0 & -R\,\sin(\psi) & R\,\cos(\psi)\,\cos(\theta) & 0 & 1 & 0 & 0 \end{pmatrix} \tag{3.18}$$

Due to the no-slip rolling conditions, which are represented by the two non-holonomic equations defined 3.17, the generalized Lagrange equation will include two Lagrange multipliers, λ_1 and λ_2.

$$L_i = \frac{d}{dt}\left(\frac{\partial L}{\partial \dot{q}_i}\right) - \frac{\partial L}{\partial q_i} = Q_i + \lambda_1 a_i + \lambda_2 b_i \tag{3.19}$$

Where a_i and b_i represent the components of the matrix A defined in 3.18. The Q_i represents the generalized mechanical actions. In our case, only the mechanical actions applied to the cylindrical joint are non-zero (Q_{i6} and Q_{i7}). These mechanical actions are associated with the generalized coordinates u and α. They will be denoted as f and τ. f represents the force at the output of the cylindrical joint, and τ represents the moment at the output of the cylindrical joint. Therefore, Q_i can be defined as follows :

$$Q_i = \begin{bmatrix} 0 & 0 & 0 & 0 & 0 & \tau & f \end{bmatrix}^T \tag{3.20}$$

The equations can be written in matrix form. M and V have been defined using MATLAB. The matrix Λ is defined as follows : $\Lambda = [\lambda_1 \ \lambda_2]^T$.

$$M(q)\,\ddot{q} + V(q, \dot{q}) = Q + A^T \Lambda \tag{3.21}$$

Where M is a 7×7positive definite symmetric matrix which represents the inertial matrix and V (7×1) contains gravity and Coriolis terms. In order to solve the dynamic equation, we will use 3.21 and the derivation of 3.17. The obtained system is written as follows :

$$\begin{cases} M(q(t))\ddot{q} + V(q, \dot{q} = Q_i + A^T \Lambda \\ \dot{A}\,\dot{q} + A\,\ddot{q} = 0 \end{cases} \tag{3.22}$$

This system can be written in matrix form as follows

$$\begin{bmatrix} M(q) & -A^T(q) \\ A(q) & 0 \end{bmatrix} \begin{bmatrix} \ddot{q} \\ \Lambda \end{bmatrix} = \begin{bmatrix} Q - V(q, \dot{q}) \\ -\dot{A}(q)\dot{q} \end{bmatrix} \tag{3.23}$$

upon setting

$$\zeta = \begin{bmatrix} M(q) & -A^T(q) \\ A(q) & 0 \end{bmatrix}, \mu = \begin{bmatrix} Q - V(q, \dot{q}) \\ -\dot{A}(q)\dot{q} \end{bmatrix}, \Gamma = \begin{bmatrix} \ddot{q} \\ \Lambda \end{bmatrix} \tag{3.24}$$

3.23 can be written as follows :

$$\zeta \Gamma = \mu \tag{3.25}$$

This equation can be solved numerically using the following relation :

$$\Gamma = \zeta^{-1} \mu \tag{3.26}$$

By integrating Γ we are able to obtain the generalized parameters and the Lagrange multipliers.

3.4.3 Reduced dynamic

Given the expected faster performance of the decoupled dynamic for model-based control and the anticipated higher accuracy of the complete dynamic, as it involves no simplifications, we introduce in this section the reduced dynamic to harness the advantages of both. To achieve this, we reduced the number of generalized parameters by eliminating the Lagrange multipliers in 3.21, and to do so, we aimed to identify a matrix 'B' that satisfies the following relationship :

$$B^T A^T = 0 \tag{3.27}$$

Upon setting and using 3.16

$$B = \begin{bmatrix} 1 & 0 & 0 & 0 & 0 \\ 0 & \frac{\cos(\psi)}{R} & \frac{\sin(\psi)}{R} & 0 & 0 \\ 0 & \frac{\sin(\psi)}{R\cos(\theta)} & -\frac{\cos(\psi)}{R\cos(\theta)} & 0 & 0 \\ 0 & 1 & 0 & 0 & 0 \\ 0 & 0 & 1 & 0 & 0 \\ 0 & 0 & 0 & 1 & 0 \\ 0 & 0 & 0 & 0 & 1 \end{bmatrix}, q_r = \begin{bmatrix} \dot{\psi} \\ \dot{x}_s \\ \dot{y}_s \\ \dot{\alpha} \\ \dot{u} \end{bmatrix} \tag{3.28}$$

The following relations are verified :

$$\begin{aligned} \dot{q} &= B\, q_r \\ B^T A^T &= 0 \end{aligned} \tag{3.29}$$

As a result, $\ddot{q}$ can be written as follow

$$\ddot{q} = \dot{B}\, q_r + B\, \dot{q}_r \tag{3.30}$$

By multiplying equation 3.21 by the transpose of matrix B, the terms related to non-holonomic constraints are eliminated. The equation becomes :

$$B^T M(q)\ddot{q} + B^T V(q, \dot{q}) = B^T Q \tag{3.31}$$

Replacing the expressions of $\dot{q}$ and $\ddot{q}$ from 3.29 and 3.30 in 3.31 we obtain the following reduced system

$$\begin{cases} \bar{M}\, \dot{q}_r + \bar{K}\, q_r + \bar{V} = Q_u \\ \dot{q} = B\, q_r \end{cases} \tag{3.32}$$

Where $\bar{M} = B^T M B$ is 5×5 matrix, $\bar{V} = B^T V$, $Q_u = B^T Q$ and $\bar{K} = B^T M \dot{B}$ are 5×1 vectors. We obtain a differential equation that can be solved numerically using this relation :

$$\dot{q}_r = \bar{M}^{-1}(Q_u - \bar{K}\, q_r - \bar{V}) \tag{3.33}$$

This method reduces the number of generalized parameters from 7 to 5.

3.5 Trajectory tracking and control

Since ARIES is a 2-DOF robot, we have control over two variables. We choose to control the X and Y cartesian positions of the center of mass of the robot. Our control strategy aims to regulate these positions to achieve accurate trajectory tracking. To facilitate this, we introduce a new variable transformation in 3.34 as our new state variable. By utilizing the dynamic models, we can express the acceleration as :

$$\begin{aligned} O &= \begin{bmatrix} X \\ Y \end{bmatrix} \\ \ddot{O} &= E(q, \dot{q}) + F(q)\gamma \end{aligned} \tag{3.34}$$

E and F are obtained from the dynamic equations by extracting the terms related to X and Y.

Here, γ encompasses the force and torque defined in Section 3. This expression proves to be invaluable for the design of our controllers.

We have adopted the same method for both the complete, reduced, and decoupled dynamics. However, in this discussion, we will focus on the expressions related to the decoupled dynamic. The dynamic model presented in 3.12 is utilized. The position mentioned in 3.34 can be obtained using the kinematic relationship presented in 3.3 :

$$\begin{aligned} X &= R\phi \\ Y &= -R\theta \end{aligned} \tag{3.35}$$

By integrating 3.35 into 3.12, we establish the relationship mentioned in 3.34, where $\gamma = [\tau\ f]$ represents the components of the transverse torques and the force exerted by the cylindrical joint. The expressions for E and F can be written as follows :

$$F = \begin{bmatrix} R(M^{-1}{}_{12} + M^{-1}{}_{13}) & RM^{-1}{}_{14} \\ -R(M^{-1}{}_{32} + M^{-1}{}_{33}) & -RM^{-1}{}_{34} \end{bmatrix}, \quad E = \begin{bmatrix} R(M^{-1}V)_1 \\ -R(M^{-1}V)_3 \end{bmatrix}$$

Here, $(M^{-1}V)_1$ and $(M^{-1}V)_3$ represent the first and third rows of the product $M^{-1}V$ and R represents the radius of the spherical shell. These terms are obtained by identification and extraction of the terms related to X and Y after applying the equation 3.35.

Due to the non-linear nature of the ARIES model, controlling the system can be challenging. After a thorough review of control strategies, we have chosen to employ sliding mode control (SMC) for this purpose. SMC is well-known for its robustness against uncertainties and disturbances, as well as its reduced sensitivity to modeling errors compared to other control strategies, as demonstrated in the next section. Furthermore, SMC is relatively straightforward to implement in a system.

The principle of SMC relies on the use of sliding surfaces and reaching laws. A sliding surface is a hypersurface defined based on the desired behavior and control objectives. The main objective of this control strategy is to drive the system to slide on this surface to reach the equilibrium point. To implement sliding mode control, we define the sliding surface as :

$$s = \frac{de}{dt} + \lambda e \tag{3.36}$$

where e is a 2×1 vector which represents the error between the measured and desired position : $e = O - O_d$. In sliding mode control, λ is used to represent a sliding mode control gain. It plays a crucial role in the design of the sliding surface and the overall behavior of the controlled system.

Therefore, we have :

$$\ddot{e} = \ddot{O} - \ddot{O}_d = E(q, \dot{q}) + F(q)\tau - \ddot{O}_d$$

The objective is to have $s = 0$. We define $\dot{s} = -K\,\text{sign}(s)$, with K a constant gain that determines the strength or intensity of the control action, the $\text{sign}(s)$ function is defined as follows :

$$\text{sign}(s) = \begin{cases} 1 & \text{if } s > 0 \\ -1 & \text{if } s < 0 \\ 0 & \text{if } s = 0 \end{cases}$$

By differentiating s and using the relation $\dot{s} = -K\,\text{sign}(s)$, we obtain :

$$\dot{s} = \ddot{e} + \lambda\dot{e} = E(q, \dot{q}) + F(q)\gamma - \ddot{O}_d + \lambda\dot{e} = -K\,\text{sign}(s)$$

The control law is then obtained as follows :

$$\gamma = F^{-1}(\ddot{O}_d - \lambda\dot{e} - E - K\,\text{sign}(s)) \tag{3.37}$$

Where F is an invertible matrix. However, the use of the sign function alone can lead to significant chattering. To reduce this chattering effect, we incorporate an enhanced exponential reaching law, as defined in 3.38 Mozayan *et al.* (2016) :

$$\dot{s} = \frac{s}{2} + \frac{K_p|s|^{\gamma}\text{sign}(s)}{\alpha - e^{-\beta|s|}(\alpha - 1)} \tag{3.38}$$

The robustness is ensured as long as K_p satisfies the relation $0 \leq K_p \leq 1$.

The block diagram of SMC is represented in Fig. 3.3

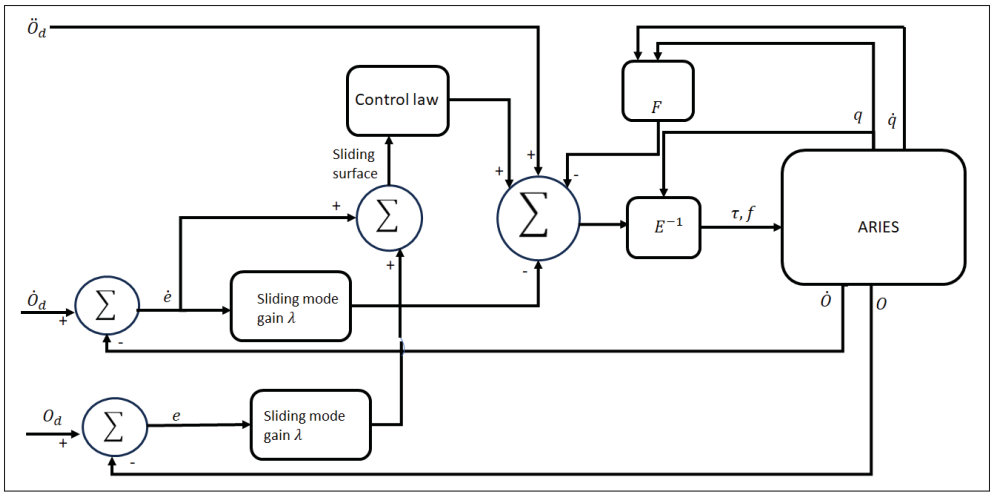

Figure 3.3 SMC block diagram

To compare SMC with another control strategy and validate our choice of using SMC, we have designed a computed torque control (CTC) approach for both the decoupled and complete dynamics of ARIES. CTC is a widely used control strategy in robotic manipulators to achieve precise and accurate control. It is a model-based control approach that leverages the dynamic model of the robot to generate control commands. We selected CTC as a basis for comparison due to its high accuracy and its similarity to SMC as a model-based control method. Additionally, CTC is relatively easy to implement and robust to parameter variations. This method is detailed in Kayacan *et al.* (2012a)

3.6 Simulation results

This section presents the simulation results for sliding mode control (SMC) and computed torque control (CTC) and also the closed loop comparison of the decoupled, reduced, and complete dynamics.

The values of the parameters used in the simulations are given in Tab.3.2. These values are obtained from the prototype of ARIES.

Tableau 3.2 Physical parameters

R	r	m_s	m_p	I_s	I_p	$\dot{\alpha}_{max}$	u_{max}	G	p
20 cm	10 cm	2 kg	7 kg	0.25 kg·m^2	0.2 kg·m^2	23.82 rad/s	3 cm	1.69	4 mm

The values of the parameters of the controllers are also displayed in Tab 3.3. We obtained these values by tuning the parameters of the controllers.

Tableau 3.3 Controller Parameters

Dynamic	**Decoupled**	**Complete**	**Reduced**
	$\lambda = \begin{bmatrix} 5 & 0 \\ 0 & 5 \end{bmatrix}$	$\lambda = \begin{bmatrix} 5 & 0 \\ 0 & 5 \end{bmatrix}$	$\lambda = \begin{bmatrix} 5 & 0 \\ 0 & 5 \end{bmatrix}$
	$\alpha = 0.02$	$\alpha = 0.03$	$\alpha = 0.04$
	$\beta = 0.5$	$\beta = 0.25$	$\beta = 0.02$
	$K_{p_1} = 0.8$	$K_{p_1} = 0.058$	$K_{p_1} = 0.2$
	$K_{p_2} = 0.1$	$K_{p_2} = 0.058$	$K_{p_2} = 0.2$

For the computed torque, the following parameters are used :

$$K_p = \begin{bmatrix} 10 & 0 \\ 0 & 5.05 \end{bmatrix}, \quad K_v = \begin{bmatrix} 10 & 0 \\ 0 & 10 \end{bmatrix} \tag{3.39}$$

These parameters are essential for accurate modeling and control of ARIES during the simulations.

3.6.1 Performance Analysis : Dynamic models

In this subsection, we conduct a closed-loop comparison between the decoupled, complete, and reduced dynamic models. As explained in Section 3, the primary distinctions between the decoupled and complete dynamics are rooted in their generalized parameter count and the

presence of non-holonomic constraints. The decoupled dynamic involves 4 variables, whereas the complete dynamic encompasses 7 variables. This differentiation arises from the separation of transverse and longitudinal movements in the decoupled dynamic, while the complete dynamic introduces added complexity through the inclusion of the Lagrange multiplier. In the case of the reduced dynamic, the primary difference from the complete dynamic is the reduction of generalized coordinates from 7 to 5. The evaluation of these dynamic models involves testing them using advanced sliding mode control. In this experiment, we utilized a circular trajectory as an input with a 1-meter radius and an angular velocity of 0.25 radians per second. The results are depicted in Figure 3.4 with the error variations in Figure 3.5. To assess the accuracy of the controllers, we calculate the root mean square error (RMSE), which measures the average magnitude of the errors between the desired and actual outputs of the system. We also calculate the maximum errors for the x and y axes for comparison purposes. The results are shown in Tab. 3.4 for comparison purposes. The findings indicate that the complete dynamic system performs better than both the decoupled and reduced dynamics specifically concerning the x position. Despite its simplification, the decoupled dynamic exhibits commendable trajectory tracking due to its ability to mitigate system non-linearities and reduce computational complexity. Similarly, the reduced dynamic achieves high accuracy compared to the complete dynamic, as it effectively streamlines computational complexity while maintaining precision.

Tableau 3.4 Performance comparison for dynamic models

Dynamics	e_{max_x}	e_{max_y}	$RMSE_x$	$RMSE_y$
Complete dynamic	3.11×10^{-4}	3.85×10^{-4}	7.1×10^{-3}	0.2198
Reduced dynamic	2.6×10^{-3}	2.3×10^{-3}	9×10^{-3}	0.2197
Decoupled dynamic	0.0132	6.79×10^{-4}	8×10^{-3}	0.229

3.6.2 Performance Analysis : Controllers type

In this subsection, we conduct a performance analysis that juxtaposes sliding mode control (SMC) and computed torque control (CTC) under identical input trajectories using decoupled and complete dynamics. The trajectories obtained for both SMC and CTC are shown in Figure

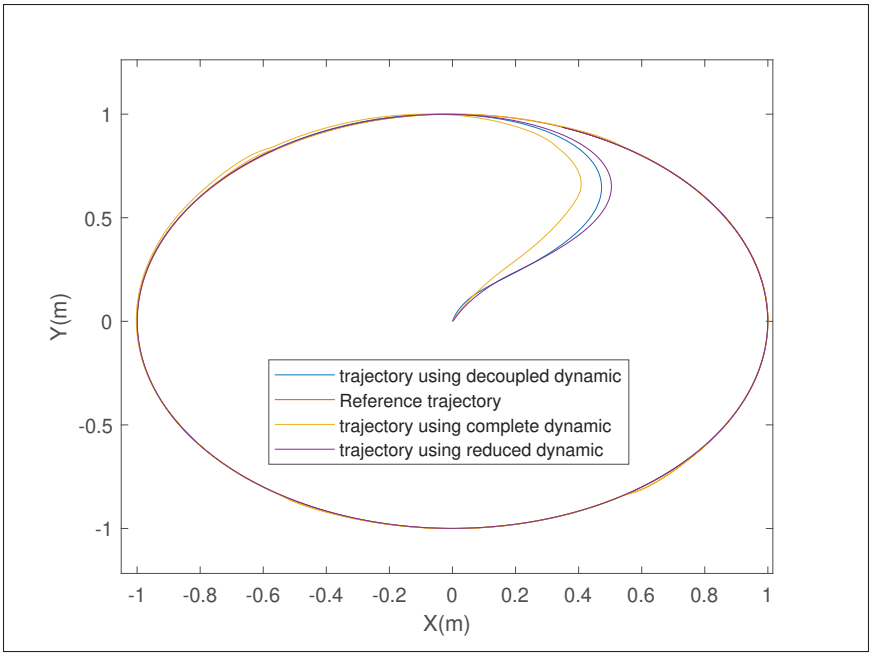

Figure 3.4 Closed loop comparison between the three dynamics

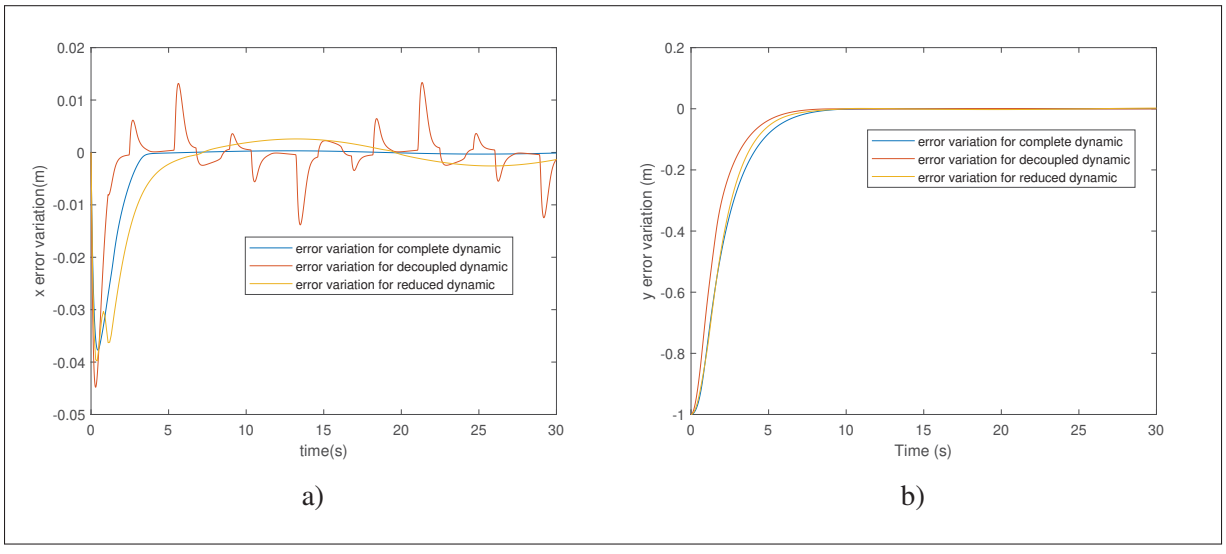

Figure 3.5 Variation of the error for decoupled, reduced and complete dynamic a shows the x-error variation over time and b shows the y-error variation over time

3.6a, with SMC demonstrating higher accuracy in trajectory tracking. We also calculated the root mean square error (RMSE) and the maximum errors for the x and y axes for comparison

purposes. The results are shown in Tab. 3.5 for comparison purposes. SMC shows superior control accuracy for the x-axis compared to CTC. Robustness assessment involves introducing model uncertainties by adding 10% of the generalized coordinate values to the system states. This evaluation aims to examine how well the controllers handle uncertainties. Figure 3.6b illustrates controller responses under these conditions, revealing SMC's capability to maintain accurate trajectory tracking even in the presence of uncertainties. In contrast, CTC faces challenges in achieving accurate tracking under uncertain conditions. An energy consumption analysis was also conducted in order to compare the controllers. Figure 3.7 illustrates the power consumption of motors for both controllers, highlighting SMC's superior energy efficiency. Considering all factors, SMC's performance and robustness, combined with its energy efficiency, position it as a superior control strategy for ARIES when compared to computed torque control (CTC).

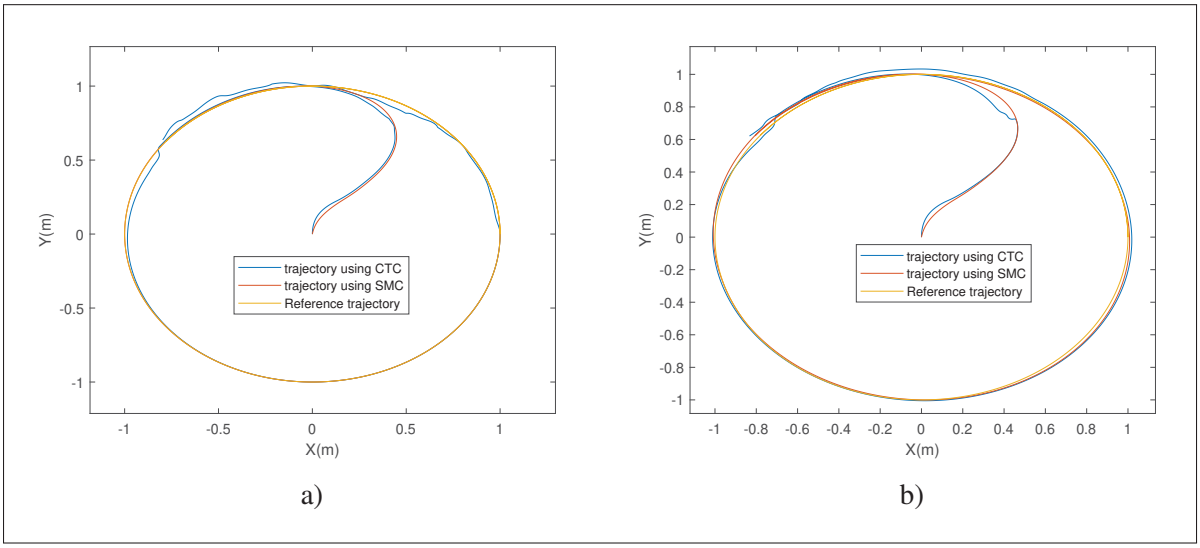

Figure 3.6 Trajectory tracking using SMC and CTC. a compare the SMC and the CTC without disturbances. The xy RSME values for SMC and CTC are 0.2036 and 0.2128 respectively. b compares SMC and the CTC with disturbances. The xy RSME values for SMC and CTC are 0.2199 and 0.2273 respectively

3.6.3 Performance Analysis : Actuation

In this section, we will compare the results obtained from the ARIES design with those derived from a more conventional design featuring a standard 2-degree-of-freedom (2-DOF) tilting

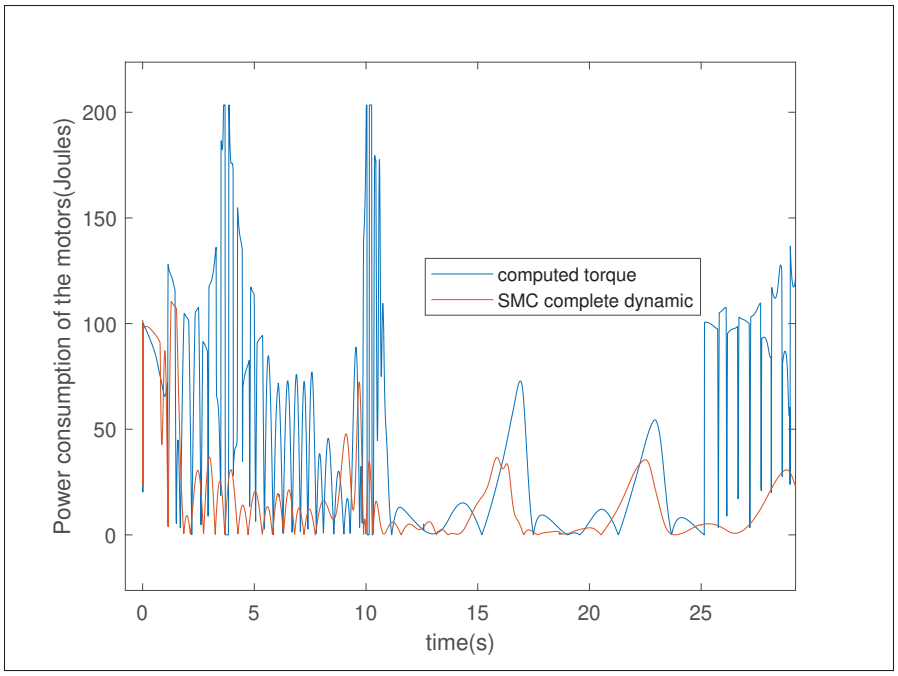

Figure 3.7 Power consumption of the motors using SMC and CTC

Tableau 3.5 Performance Comparison : SMC vs. CTC

Controller	e_{max_x}	e_{max_y}	$RMSE_x$	$RMSE_y$
SMC	3.11×10^{-4}	3.8532×10^{-4}	7.1×10^{-3}	0.2198
CTC	4.8×10^{-4}	0.0387	0.0120	0.2290

mechanism. The primary distinction between these two mechanisms lies in the nature of the tilting action : while ARIES generates a translational motion, the more traditional design produces a rotational one. To facilitate a meaningful comparison, we maintained consistent parameters with those used in ARIES. In the 2-DOF tilting mechanism, the translational output u is replaced by an angular variable β As demonstrated in experiments conducted in Belzile & St-Onge (2022b), a maximum translation of $u = 3cm$ corresponds to a maximum rotation of $\beta = 39$ deg. We utilized a well-established model introduced by Kayacan et al. Kayacan *et al.* (2012a), incorporating ARIES parameters. Additionally, we implemented our custom sliding mode control approach for a comparative analysis. Both the established model and our approach were subjected to the same

input : a circular trajectory with a 0.5m radius and an angular velocity of 0.5rad/s. The resulting trajectory when using sliding mode control is illustrated in Fig. 3.8a, demonstrating that both designs exhibit excellent trajectory tracking.

In Fig. 3.9, we have presented plots of u and β over time. These plots reveal an interesting distinction between the two designs. The cylindrical drive design requires minimal tilting, while the double pendulum design necessitates a maximum rotation of β to achieve the same trajectory. This disparity in motion reflects differences in power consumption, as depicted in Fig.3.8b. Notably, the cylindrical drive design proves to be more energy-efficient in achieving the desired trajectory.

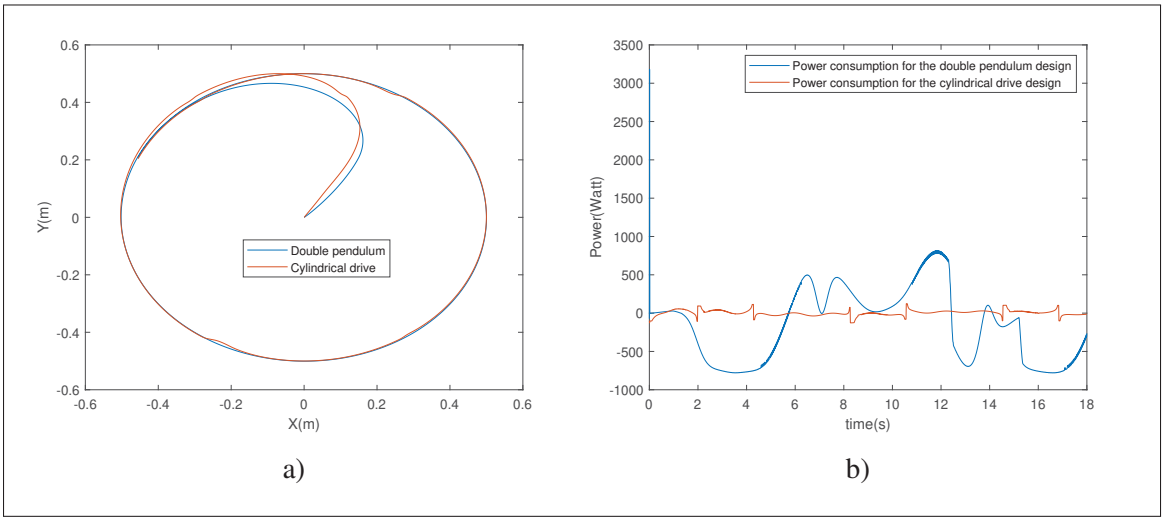

Figure 3.8 Comparison between the double pendulum and cylindrical drive designs a shows the trajectory following and b shows the power consumption of the motors for the designs

3.7 Hardware implementation

In the next study, we will evaluate the performance of our designed controllers, we will conduct experiments using a physical prototype of ARIES. ARIES is characterized by a cylindrical drive mechanism enclosed within a transparent polycarbonate shell divided into two hemispheres. A hermetic seal is ensured through an overlapping section, and the shell's curvature is tailored to accommodate two Maxon brushless DC motors equipped with hall sensors and two quadrature

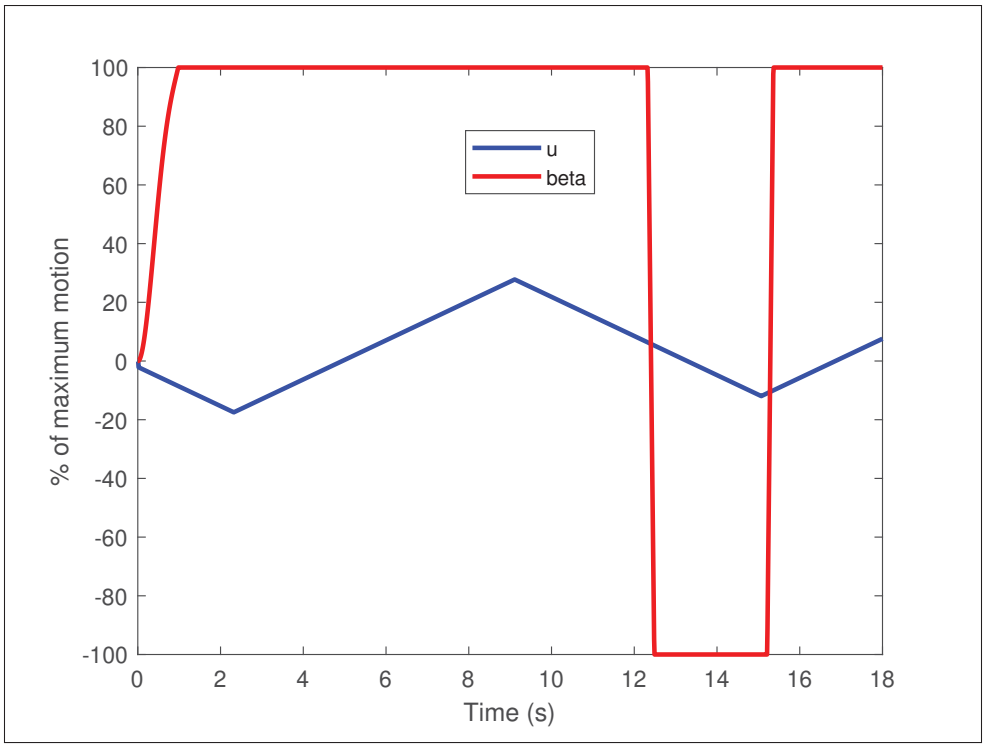

Figure 3.9 percentage of the maximum motion for the cylindrical drive and the double pendulum in function of the time

encoders. These motor components facilitate the measurement of motor rotation, enabling us to determine both the translation and rotation of the cylindrical joint. Additionally, we will employ an ultra-wideband (UWB) system containing an inertial measurement unit sensor and a Kalman filter to precisely ascertain the position and orientation of the sphere's center of mass.

For motor control, we will utilize the transpose of the Jacobian matrix J, which is defined as follows :

$$J = \begin{bmatrix} 2\pi & pG \\ -2\pi & pG \end{bmatrix} \tag{3.40}$$

The transpose of this Jacobian matrix will allow us to compute the generalized forces τ and f, as mentioned earlier, using the equation :

$$\begin{bmatrix} \tau \\ f \end{bmatrix} = J^T \begin{bmatrix} \tau_L \\ \tau_R \end{bmatrix} \tag{3.41}$$

Here, τ_L and τ_R represent the torque applied to the left and right motors, respectively.

Furthermore, the motor controllers we intend to use operate based on voltage inputs, necessitating two conversions. The first conversion translates torque to voltage using the following formula :

$$n = K_w \cdot U_{\text{mot}} - \frac{\delta_n}{\delta_m} \cdot \tau \tag{3.42}$$

Where :

- K_w is the speed constant of the motors. - $\frac{\delta_n}{\delta_m}$ is the speed-to-torque gradient of the motors. - U_{mot} is the power voltage supplied to the motors. - τ represents the torque applied to the motors.

The second conversion relates to translating speed into voltage, as follows :

$$V_{\text{set}} = \frac{n - n_{\text{min}}}{n_{\text{max}} - n_{\text{min}}} \cdot 4.9 + 0.1 \tag{3.43}$$

In this equation :

- n denotes the velocity of the motors. - n_{min} and n_{max} correspond to the minimum and maximum velocities, respectively.

The robot is equipped with a Xavier Jetson microcontroller running the Robot Operating System (ROS). To send velocity commands from the controllers to the robot, we employ subscriber and publisher blocks in Simulink. The publisher block is named "cmdVel," and it sends velocity commands to the motor controllers. To obtain the feedback information necessary for control, we use three publishers :

1. "Pose," which provides filtered position data of the robot as well as quaternions to determine its orientation. This information is obtained from the UWB sensor.

2. "Vel," which gives filtered linear and angular velocities of the robot, is also derived from the UWB sensor.

3. "Robot states," which supplies translational and rotational outputs α and u and their derivatives, obtained using the encoders. Low-pass filters have been added in Simulink to reduce noise in this data. The architecture of the system is summarized in Figure 3.10.

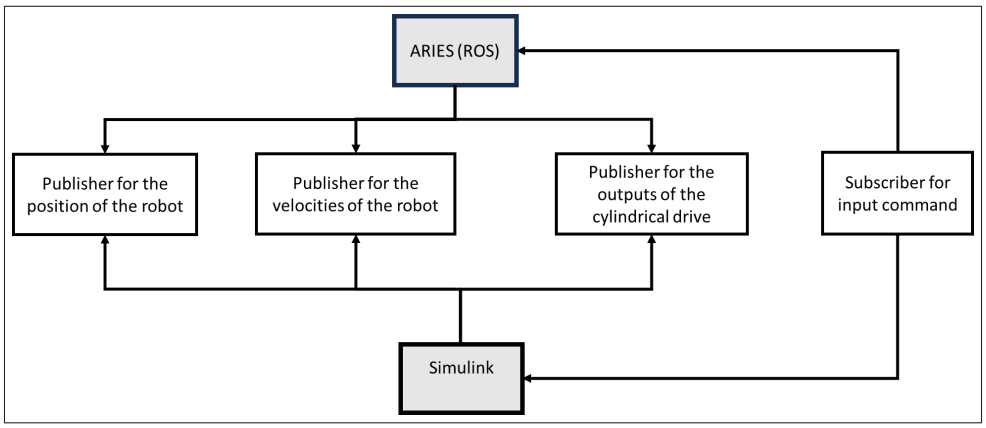

Figure 3.10 Data flow for direct control of ARIES

To validate our dynamic models, we conducted real-world experiments with the robot in an open loop. We applied a one-volt input voltage to both motors, equivalent to a torque of 0.3 N·m and zero force. We also fed the same input voltage to the model, both on the real robot and in Simulink using a publisher.

The results of this comparison can be seen in Figure 3.11. In these figures, a compares the x-position of the robot with the complete dynamic model, and b compares the y-position of the model with the complete dynamic model.

As evident from our observations, there is a strong resemblance between the simulation outcomes and real-world outcomes, confirming the accuracy of our dynamic modeling. It's essential to take

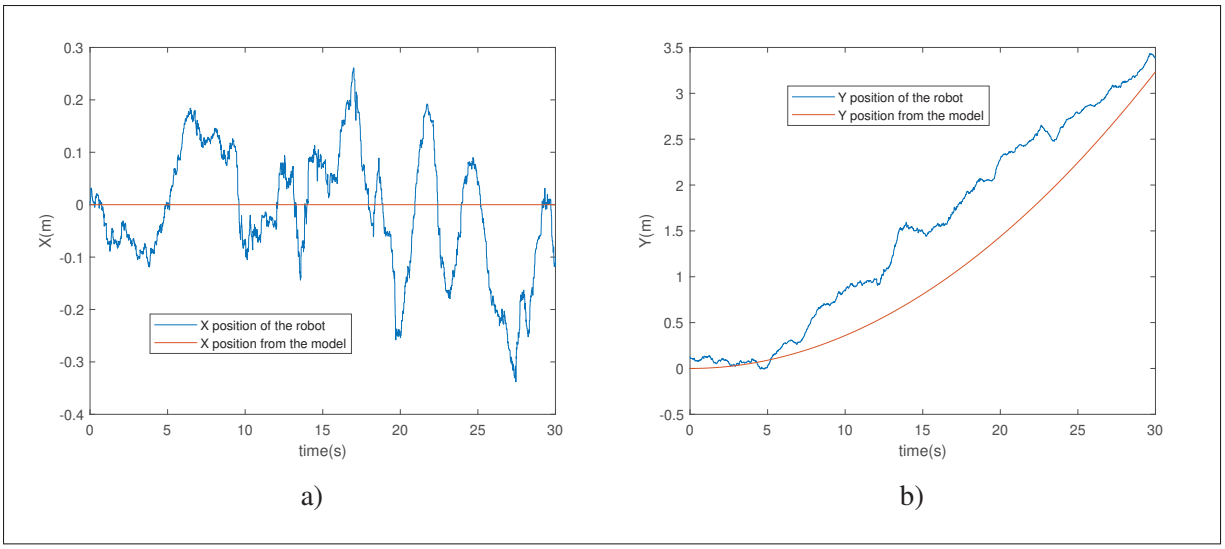

Figure 3.11 Open loop validation a compares the x-position of the robot with the complete dynamic model, and b compares the y-position of the model with the complete dynamic model

into account potential discrepancies related to the 10 cm precision of the UWB (Ultra-Wideband) technology, particularly concerning the y-axis.

It's also worth noting that wobbling is visible in the y-position of the robot. This wobbling is expected to be mitigated by the controller. Such oscillations are primarily caused by inertial effects. Specifically, rapid changes in direction induce wobbling as the robot's mass resists alterations in its motion state, primarily due to its moment of inertia.

3.8 Conclusion

In this study, we investigated the modeling, analysis, and control aspects of spherical robots, with a particular focus on ARIES—a 2-degree-of-freedom (2-DOF) pendulum robot capable of both rolling and tilting motions around the sphere's axis. We proposed three distinct ways of modeling ARIES using the Lagrange method :

The first approach involved considering the full dynamics of the system without simplifications, providing a comprehensive understanding of its behavior.

The second approach decoupled the transversal and longitudinal axes, treating them as independent dynamics, which allowed for a more focused examination of each axis's behavior.

The third approach employed a variable transformation to reduce the complete dynamics from 7 to 5 variables, simplifying the model while retaining essential characteristics.

We conducted simulation experiments using Simulink to compare the performance of these dynamic modeling approaches. Sliding mode control was employed, and various metrics were used for evaluation. The outcomes revealed the efficiency of the complete dynamic model in terms of accuracy, compared to the decoupled and reduced dynamic. Furthermore, a comparison between sliding mode control and computed torque control was conducted to assess the robustness and accuracy of sliding mode control. The findings revealed that sliding mode control outperformed computed torque control for ARIES, displaying greater robustness to uncertainties.

Additionally, this study compared actuation mechanisms by utilizing a double pendulum model with parameters analogous to those of ARIES. The double pendulum model was subjected to sliding mode control, facilitating a comparative analysis.

Looking ahead, the next phase of this research involves conducting experiments on the physical prototype of ARIES to validate these strategies in real-time scenarios, thus bridging the gap between simulation and practical application.

Acknowledgment

We would like to express our gratitude to Bruno Belzile and Simon Bonneau for their valuable support during this research process

Funding Data

- NSERC Discovery Grant (RGPIN-2020-06121)
- Canadian Space Agency (CSAFAST 19FAPOLA32).

CONCLUSION ET RECOMMANDATIONS

Les principaux objectifs de cette recherche étaient de développer des stratégies de contrôle robustes pour la modélisation et le contrôle d'ARIES, tout en réalisant une analyse comparative de trois approches distinctes de modélisation dynamique et de deux stratégies de contrôle.

Pour atteindre ces objectifs, notre étude a débuté par une revue exhaustive de l'état actuel des robots sphériques, couvrant divers aspects tels que la conception, la locomotion, le contrôle et l'intégration de capteurs. Cette revue nous a fourni des informations précieuses qui ont jeté les bases de notre recherche spécifique sur ARIES.

Au cours de cette revue approfondie, nous avons identifié 33 stratégies de contrôle utilisées dans le domaine, avec le contrôle basé sur le mode de glissement émergent comme le choix dominant. Cela a mis en évidence la robustesse et la précision de la méthode par mode de glissement dans le contrôle d'ARIES.

En ce qui concerne la modélisation dynamique, nous avons exploré diverses approches et conclu que le modèle dynamique complet dépassait les modèles simplifiés en termes de précision, tandis que les modèle découplés et reduits réduisaient la complexité de calcul.

Cette recherche a également démontré l'efficacité du contrôle par glissement par rapport au contrôle par couple calculé.

Notre recherche met en évidence l'importance cruciale de l'innovation continue dans la technologie des robots sphériques, une discipline qui s'avère être au cœur des avancées dans l'exploration spatiale. Dans cette étude, nous faisons une contribution significative au domaine de l'exploration spatiale, en nous concentrant spécifiquement sur l'exploration des cavernes lunaires. Les robots sphériques se sont imposés comme des outils inestimables dans cette quête, et leur rôle ne cesse de s'amplifier. Les cavernes lunaires représentent un environnement extrêmement inhospitalier et peu exploré. Elles sont pleines de mystères et de possibilités,

mais aussi de dangers potentiels. Dans ce contexte, les robots sphériques se révèlent être des partenaires idéaux.

L'une des clés de leur efficacité réside dans notre capacité à innover continuellement dans la conception, la modélisation et le contrôle de ces robots. Nous devons développer des technologies avancées qui leur permettent de naviguer de manière autonome dans les cavernes, de cartographier ces espaces complexes et potentiellement dangereux, et de recueillir des données essentielles pour notre compréhension de la Lune et de son histoire. Cette recherche contribue non seulement à la science fondamentale de l'exploration spatiale, mais elle a également des implications pratiques pour les missions futures. Grâce à l'innovation continue dans la technologie des robots sphériques, nous sommes mieux préparés que jamais à relever le défi passionnant de l'exploration des cavernes lunaires et à élargir notre compréhension de l'univers qui nous entoure.

Dans le cadre de nos travaux futurs, nous prévoyons de mettre en œuvre les stratégies de contrôle identifiées dans un prototype d'ARIES afin de valider les résultats obtenus à partir de Simulink, établissant ainsi un lien entre la simulation et l'application pratique. De plus, nous envisageons la création de plusieurs prototypes d'ARIES pour former une flotte de robots qui sera déployée sur la lune dans le but de cartographier et de localiser les cavernes lunaires.

BIBLIOGRAPHIE

Ajay, V. A., Suherlan, A. P., Soh, G. S., Foong, S., Wood, K. & Otto, K. (2015). Localization and trajectory tracking of an autonomous spherical rolling robot using imu and odometry. *ASME 2015 International Design Engineering Technical Conferences and Computers and Information in Engineering Conference, IDETC/CIE 2015, August 2, 2015 - August 5, 2015*, 5A-2015(Proceedings of the ASME Design Engineering Technical Conference), Computers and Information in Engineering Division ; Design Engineering Division. doi : 10.1115/DETC2015-47223.

Alves, J. & Dias, J. (2003). Design and control of a spherical mobile robot. *Proceedings of the Institution of Mechanical Engineers, Part I : Journal of Systems and Control Engineering*, 217(6), 457–467. doi : 10.1177/095965180321700602.

Andani, M. T., Shahmiri, S., Pourgharibshahi, H., Yousefpour, K., Imani, M. H. & IEEE. (2018). Fuzzy-Based Sliding Mode Control and Sliding Mode Control of a Spherical Robot. *IECON 2018 - 44TH ANNUAL CONFERENCE OF THE IEEE INDUSTRIAL ELECTRONICS SOCIETY*, pp. 2534–2539. Repéré à http://dx.doi.org/10.1109/IECON.2018.8591640.

Armour, R. H. & Vincent, J. F. V. (2006a). Rolling in Nature and Robotics : A Review. *Journal of Bionic Engineering*, 3(4), 195–208. doi : 10.1016/S1672-6529(07)60003-1.

Armour, R. H. & Vincent, J. F. V. (2006b). Rolling in Nature and Robotics : A Review. *Journal of Bionic Engineering*, 3(4), 195–208. doi : 10.1016/S1672-6529(07)60003-1.

Asiri, S., Khademianzadeh, F., Monadjemi, A. & Moallem, P. (2019). The Design and Development of a Dynamic Model of a Low-Power Consumption, Two-Pendulum Spherical Robot. *IEEE/ASME Transactions on Mechatronics*, 24(5), 2406–2415. doi : 10.1109/TMECH.2019.2934180.

Ayati, M. & Zarei, S. (2017). *Fault Detection Algorithm based on Sliding-mode method for spherical Rolling Robots*. The Institute of Electrical and Electronics Engineers, Inc. (IEEE) Conference Proceedings. Institute of Electrical and Electronics Engineers Inc.

Azizi, M. & Keighobadi, J. (2014). Robust Sliding Mode Trajectory Tracking Controller for a Nonholonomic Spherical Mobile Robot. *IFAC Proceedings Volumes*, 47(3), 4541–4546. doi : 10.3182/20140824-6-ZA-1003.01430.

Balandin, D., Komarov, M. & Osipov, G. (2013). A motion control for a spherical robot with pendulum drive. *JOURNAL OF COMPUTER AND SYSTEMS SCIENCES INTERNATIONAL*, 52(4), 650–663. doi : 10.1134/S1064230713040047.

Bastola, S. & Zargarzadeh, H. (2019). Super Twisting Sliding Mode Control of Spherical Robot. *2019 IEEE INTERNATIONAL SYMPOSIUM ON MEASUREMENT AND CONTROL IN ROBOTICS (ISMCR) : ROBOTICS FOR THE BENEFIT OF HUMANITY*. Repéré à http://dx.doi.org/10.1109/ISMCR47492.2019.8955701.

Behar, A., Carsey, F., Matthews, J. & Jones, J. (2004). NASA/JPL tumbleweed polar rover. *IEEE Aerospace Conference Proceedings*, 1, 388–395. doi : 10.1109/aero.2004.1367622.

Belskii, G. & Serykh, E. (2021). *Spherical Robot Remote Control Development*. The Institute of Electrical and Electronics Engineers, Inc. (IEEE) Conference Proceedings. Institute of Electrical and Electronics Engineers Inc.

Belskii, G. V., Serykh, E. V. & Pankratev, D. A. (2021). Design and Implementations of Spherical Robot Hardware Level. *The Institute of Electrical and Electronics Engineers, Inc. (IEEE) Conference Proceedings*, 806–809. doi : 10.1109/ElConRus51938.2021.9396257.

Belzile, B. & St-Onge, D. (2022a). Design and Modeling of a Spherical Robot Actuated by a Cylindrical Drive. *2022 International Conference on Robotics and Automation (ICRA)*, pp. 1169-1175. doi : 10.1109/ICRA46639.2022.9812148.

Belzile, B. & St-Onge, D. (2022b). ARIES : Cylindrical Pendulum Actuated Explorer Sphere. *IEEE/ASME Transactions on Mechatronics*, 27(4), 2142-2150. doi : 10.1109/TMECH.2022.3175989.

Bhattacharya, S. & Agrawal, S. K. (2000). Spherical rolling robot : A design and motion planning studies. *IEEE Transactions on Robotics and Automation*, 16(6), 835–839. doi : 10.1109/70.897794.

Bowkett, J., Burkhardt, M. & Burdick, J. W. (2017). Combined Energy Harvesting and Control of Moball : A Barycentric Spherical Robot. *Springer Proceedings in Advanced Robotics*, 1, 71–83. doi : 10.1007/978-3-319-50115-4_7.

Cai, Y., Zhan, Q. & Xi, X. (2011). Neural network control for the linear motion of a spherical mobile robot. *International Journal of Advanced Robotic Systems*, 8(4), 79–87. doi : 10.5772/45711.

Cai, Y., Zhan, Q. & Xi, X. (2012). Path tracking control of a spherical mobile robot. *Mechanism and Machine Theory*, 51, 58–73. doi : 10.1016/j.mechmachtheory.2011.12.009.

Chase, R. (2014). *Analysis Of A Dual Scissored-Pair, Variable-Speed, Control Moment Gyroscope Driven Spherical Robot*. (Thèse de doctorat).

Chase, R. & Pandya, A. (2012). A Review of Active Mechanical Driving Principles of Spherical Robots. *Robotics*, 1(1), 3–23. doi : 10.3390/robotics1010003.

Chen, J., Ye, P., Sun, H. & Jia, Q. (2017, 1). Design and motion control of a spherical robot with control moment gyroscope. *2016 3rd International Conference on Systems and Informatics, ICSAI 2016*, pp. 114–120. doi : 10.1109/ICSAI.2016.7810940.

Chen, S. B., Beigi, A., Yousefpour, A., Rajaee, F., Jahanshahi, H., Bekiros, S., Martinez, R. A. & Chu, Y. M. (2020). Recurrent Neural Network-Based Robust Nonsingular Sliding Mode Control With Input Saturation for a Non-Holonomic Spherical Robot. *IEEE ACCESS*, 8, 188441–188453. doi : 10.1109/ACCESS.2020.3030775.

Chiu, C.-W., Wang, C.-H. & Hwang, C.-K. (2012). Hierarchical sliding mode control of a spherical robot driven by Omni wheels. 4(Proceedings - International Conference on Machine Learning and Cybernetics), 1612–1616. doi : 10.1109/ICMLC.2012.6359606.

Chowdhury, A. R., Soh, G. S., Foong, S. & Wood, K. L. (2018a). Implementation of Caterpillar Inspired Rolling Gait and Nonlinear Control Strategy in a Spherical Robot. *JOURNAL OF BIONIC ENGINEERING*, 15(2), 313–328. doi : 10.1007/s42235-018-0024-x.

Chowdhury, A. R., Vibhute, A., Soh, G. S., Foong, S. H. & Wood, K. L. (2017). Implementing caterpillar inspired roll control of a spherical robot.

Chowdhury, A. R., Soh, G. S., Foong, S. H. & Wood, K. L. (2018b). Experiments in robust path following control of a rolling and spinning robot on outdoor surfaces. *Robotics and Autonomous Systems*, 106, 140–151. doi : 10.1016/j.robot.2018.05.004.

Chowdhury, A. R., Soh, G. S., Foong, S. H., Wood, K. L. & IEEE. (2018c). Evaluating Robust Trajectory Control of a Miniature Rolling and Spinning Robot in Outdoor Conditions.

DeJong, B. P., Karadogan, E., Yelamarthi, K. & Hasbany, J. (2017). Design and Analysis of a Four-Pendulum Omnidirectional Spherical Robot. *J Intell Robot Syst*, 86, 3–15. doi : 10.1007/s10846-016-0414-4.

Diouf, A., Belzile, B., Saad, M. & St-Onge, D. (2023). Spherical Rolling Robots Design, Modeling, and Control : A Systematic Literature Review. (arXiv :2310.02240). Repéré à http://arxiv.org/abs/2310.02240. arXiv :2310.02240 [cs].

Ghanbari, A., Mahboubi, S. & Fakhrabadi, M. M. S. (2010). Design, dynamic modeling and simulation of a spherical mobile robot with a novel motion mechanism. *Proceedings of 2010 IEEE/ASME International Conference on Mechatronic and Embedded Systems and Applications, MESA 2010*, pp. 434–439. doi : 10.1109/MESA.2010.5551991.

Ghommam, J., Mahmoud, M. S. & Saad, M. (2013). Robust cooperative control for a group of mobile robots with quantized information exchange. *Journal of the Franklin Institute*, 350(8), 2291–2321. doi : 10.1016/j.jfranklin.2013.05.031.

Guan, X. Q., Zhang, M., Wu, R. M., Gao, H., Ai, Q., Jin, S., Wang, Y., Li, G. & IEEE. (2020). Remote Control System of Spherical Robot based on Silent Speech Recognition. *2020 8TH INTERNATIONAL WINTER CONFERENCE ON BRAIN-COMPUTER INTERFACE (BCI)*, pp. 212–217.

Halme, A., Schonberg, T. & Wang, Y. (1996). Motion control of a spherical mobile robot. *International Workshop on Advanced Motion Control, AMC*, 1, 259–264. doi : 10.1109/amc.1996.509415.

Hanxu, S., Yili, Z. & Qingxuan, J. (2010). Dymanics analysis and control method of a novel spherical robot. (Proceedings of the ASME Dynamic Systems and Control Conference 2009, DSCC2009), 1683–1688.

Hu, T., Guan, X., Lin, B., Wang, Y., Liu, Y., Wang, Y. & Li, G. (2022). Optimal Velocity Control of Spherical Robots Based on Offset-free Linear Model Predictive Control. pp. 363–368.

Huang, K.-S., Lin, Y.-H., Lin, K.-B., Lee, B.-K. & Hwang, C.-K. (2012). Cascade sliding mode control of a spherical wheel robot driven by Omni wheels. *2012 International Conference on Machine Learning and Cybernetics, ICMLC 2012, July 15, 2012 - July 17, 2012*, 4(Proceedings - International Conference on Machine Learning and Cybernetics), 1607–1611. doi : 10.1109/ICMLC.2012.6359605.

Huang, Y., Zhu, G., Wang, C., Huang, H. & Inc, D. P. (2017). Dynamical Modelling and Positioning Control Simulation of a Spherical Robot Driven by Three Omnidirectional Wheels. pp. 157–164.

Jaimez, M., Castillo, J. J., García, F. & Cabrera, J. A. (2012). Design and Modelling of Omnibola, A Spherical Mobile Robot. *Mechanics Based Design of Structures and Machines*, 40(4), 383–399. doi : 10.1080/15397734.2012.687285.

Javadi, A. H. A. & Mojabi, P. (2002). Introducing August : A novel strategy for an omnidirectional spherical rolling robot. *Proceedings-IEEE International Conference on Robotics and Automation*, 4, 3527–3533. doi : 10.1109/ROBOT.2002.1014256.

Jayoung, K., Hyokjo, K. & Jihong, L. (2009). A rolling robot : Design and implementation. *2009 7th Asian Control Conference, ASCC 2009, August 27, 2009 - August 29, 2009*, (Proceedings of 2009 7th Asian Control Conference, ASCC 2009), 1474–1479.

Jia, Q., Zheng, Y., Sun, H., Cao, H. & Li, H. (2009). Motion control of a novel spherical robot equipped with a flywheel. *2009 IEEE International Conference on Information and Automation, ICIA 2009*, pp. 893–898. doi : 10.1109/ICINFA.2009.5205045.

Joshi, V. A. & Banavar, R. N. (2009). Motion analysis of a spherical mobile robot. *Robotica*, 27(3), 343–353. doi : 10.1017/S0263574708004748.

Kalita, H., Gholap, A. S. & Thangavelautham, J. (2020). *Dynamics and Control of a Hopping Robot for Extreme Environment Exploration on the Moon and Mars*. The Institute of Electrical and Electronics Engineers, Inc. (IEEE) Conference Proceedings. IEEE Computer Society.

Kamaldar, M., Mahjoob, M., Yazdi, M. H., Vahid-Alizadeh, H. & Ahmadizadeh, S. (2011a). A control synthesis for reducing lateral oscillations of a spherical robot. *2011 IEEE International Conference on Mechatronics, ICM 2011 - Proceedings*, (2011 IEEE International Conference on Mechatronics, ICM 2011 - Proceedings), 546–551. doi : 10.1109/ICMECH.2011.5971346.

Kamaldar, M., M.J., M. & H., V. A. (2011b). Robust speed control of a spherical robot using ARX uncertain modeling. pp. 196–201. doi : 10.1109/ROSE.2011.6058538.

Karavaev, Y., Mamaev, I., Kilin, A. & Pivovarova, E. (2020). Spherical rolling robots : Different designs and control algorithms. (Robots in Human Life- Proceedings of the 23rd International Conference on Climbing and Walking Robots and the Support Technologies for Mobile Machines, CLAWAR 2020), 195–202. doi : 10.13180/clawar.2020.24-26.08.47.

Kayacan, E., Bayraktaroglu, Z. Y. & Saeys, W. (2012a). Modeling and control of a spherical rolling robot : A decoupled dynamics approach. *Robotica*, 30(4), 671–680. doi : 10.1017/S0263574711000956.

Kayacan, E., Kayacan, E., Ramon, H. & Saeys, W. (2012b). Velocity Control of a Spherical Rolling Robot Using a Grey-PID Type Fuzzy Controller With an Adaptive Step Size. *10th IFAC Symposium on Robot Control*, 45(22), 863–868. doi : 10.3182/20120905-3-HR-2030.00123.

Kayacan, E., Kayacan, E., Ramon, H. & Saeys, W. (2013). Adaptive neuro-fuzzy control of a spherical rolling robot using sliding-mode-control-theory-based online learning algorithm. *IEEE Transactions on Cybernetics*, 43(1), 170–179. doi : 10.1109/TSMCB.2012.2202900.

Kolbari, H., Ahmadi, A., Bahrami, M., Janati, F. & Ardekany, A. N. (2018). Impedance Estimation and Motion Control of a Pendulum-Driven Spherical Robot. *2018 6TH RSI INTERNATIONAL CONFERENCE ON ROBOTICS AND MECHATRONICS (ICROM 2018)*, pp. 6–11. Repéré à http://dx.doi.org/10.1109/ICRoM.2018.8657621.

Landa, K. & Pilat, A. K. (2015, 8). Design and start-up of spherical robot with internal pendulum. *2015 10th International Workshop on Robot Motion and Control, RoMoCo 2015*, pp. 27–32. doi : 10.1109/RoMoCo.2015.7219709.

Li, B., Deng, Q. & Liu, Z. (2009). A spherical hopping robot for exploration in complex environments. *2009 IEEE International Conference on Robotics and Biomimetics, ROBIO 2009*, pp. 402–407. doi : 10.1109/ROBIO.2009.5420680.

Li, W. & Zhan, Q. (2018). Kinematics Based Sliding-Mode Control for Trajectory Tracking of a Spherical Mobile Robot.

Li, W. & Zhan, Q. (2019). Kinematics-based four-state trajectory tracking control of a spherical mobile robot driven by a 2-DOF pendulum. *Chinese Journal of Aeronautics*, 32(6), 1530–1540. doi : 10.1016/j.cja.2018.09.002.

Li, Y. (2020). Anti-disturbance Control of Vertical Pitch Attitude of Underwater Spherical Robot. *The Institute of Electrical and Electronics Engineers, Inc. (IEEE) Conference Proceedings*, 6–11. doi : 10.1109/RCAE51546.2020.9294502.

Lin, X. & Guo, S. (2012). Development of a spherical underwater robot equipped with multiple vectored water-jet-based thrusters. *Journal of Intelligent and Robotic Systems : Theory and Applications*, 67(3-4), 307–321. doi : 10.1007/s10846-012-9651-3.

Ling, Z., Zhang, J., Weng, R., Cai, B., Li, B., Zhang, S. & Xiao, G. (2022). A Dynamic-Model-Based Predictive Controller for a Novel Pendulum-Driven Spherical Robot. *7th International Conference on Robotics and Automation Engineering, ICRAE 2022, November 18, 2022 - November 20, 2022*, (2022 7th International Conference on Robotics and Automation Engineering, ICRAE 2022), 191–198. doi : 10.1109/ICRAE56463.2022.10056223.

Liu, D. L. & Sun, H. X. (2010). Nonlinear Sliding-mode Control for Motion of a Spherical Robot. *PROCEEDINGS OF THE 29TH CHINESE CONTROL CONFERENCE*, pp. 3244–3249.

Liu, D. L., Sun, H. X., Jia, Q. X. & IEEE. (2008). Stabilization and Path Following of a Spherical Robot. *2008 IEEE CONFERENCE ON ROBOTICS, AUTOMATION, AND MECHATRONICS, VOLS 1 AND 2*, pp. 196–202. Repéré à http://dx.doi.org/10.1109/RAMECH.2008.4681358.

Liu, D., Sun, H. & Jia, Q. (2009). A Family of Spherical Mobile Robot : Driving Ahead Motion Control by Feedback Linearization. *ISSCAA2008 : The 2nd International Symposium on Systems and Control in Aeronautics and Astronautics*, 80.

Liu, Y., Wang, Y., Guan, X., Wang, Y., Jin, S., Hu, T., Ren, W., Hao, J., Zhang, J. & Li, G. (2022). Multi-Terrain Velocity Control of the Spherical Robot by Online Obtaining the Uncertainties in the Dynamics. *IEEE Robotics and Automation Letters*, 7(2), 2732-2739. doi : 10.1109/LRA.2022.3141210.

Ma, L., Sun, H. & Song, J. (2020). Fractional-Order Adaptive Integral Hierarchical Sliding Mode Control Method for High-Speed Linear Motion of Spherical Robot. *IEEE Access*, 8, 66243–66256. doi : 10.1109/ACCESS.2020.2985380.

Mizumura, Y., Ishibashi, K., Yamada, S., Takanishi, A. & Ishii, H. (2018). Mechanical design of a jumping and rolling spherical robot for children with developmental disorders. *2017 IEEE International Conference on Robotics and Biomimetics, ROBIO 2017*, 2018-Janua, 1–6. doi : 10.1109/ROBIO.2017.8324558.

Mozayan, S. M., Saad, M., Vahedi, H., Fortin-Blanchette, H. & Soltani, M. (2016). Sliding Mode Control of PMSG Wind Turbine Based on Enhanced Exponential Reaching Law. *IEEE Transactions on Industrial Electronics*, 63(10), 6148–6159. doi : 10.1109/TIE.2016.2570718.

Mukherjee, R., Minor, M. A. & Pukrushpan, J. T. (1999). Simple motion planning strategies for spherobot : a spherical mobile robot. *Proceedings of the IEEE Conference on Decision and Control*, 3, 2132–2137. doi : 10.1109/cdc.1999.831235.

Muralidharan, V. & Mahindrakar, A. D. (2015). Geometric controllability and stabilization of spherical robot dynamics. *IEEE Transactions on Automatic Control*, 60(10), 2762–2767. doi : 10.1109/TAC.2015.2404512.

Nakashima, A., Maruo, S., Nagai, R. & Sakamoto, N. (2018). 2-Dimensional Dynamical Modeling and Control of Spherical Robot Driven by Inner Car. *The Institute of Electrical and Electronics Engineers, Inc. (IEEE) Conference Proceedings*, 1846–1851.

Nam, D. W., Lee, C., Choi, J., Kim, Y. & Lee, S.-G. (2019). Deep Learning Approach for Linear Locomotion Control of Spherical Robot. *The Institute of Electrical and Electronics Engineers, Inc. (IEEE) Conference Proceedings*, 557–562. doi : 10.23919/ICCAS47443.2019.8971544.

Nguyen, V. D., Soh, G. S., Foong, S. & Wood, K. (2017). *De-coupled dynamics control of a spherical rolling robot for waypoint navigation*. The Institute of Electrical and Electronics Engineers, Inc. (IEEE) Conference Proceedings. Institute of Electrical and Electronics Engineers Inc.

Niu, X., Suherlan, A. P., Soh, G. S., Foong, S., Wood, K. & Otto, K. (2014). Mechanical Development and Control of a Miniature Nonholonomic Spherical Rolling Robot. *2014 13th International Conference on Control Automation Robotics & Vision (ICARCV)*, 2014(December), 1923–1928. doi : 10.1109/ICARCV.2014.7064610.

Page, M. J., McKenzie, J. E., Bossuyt, P. M., Boutron, I., Hoffmann, T. C., Mulrow, C. D., Shamseer, L., Tetzlaff, J. M., Akl, E. A., Brennan, S. E., Chou, R., Glanville, J., Grimshaw, J. M., Hróbjartsson, A., Lalu, M. M., Li, T., Loder, E. W., Mayo-Wilson, E., McDonald, S., McGuinness, L. A., Stewart, L. A., Thomas, J., Tricco, A. C., Welch, V. A., Whiting, P. & Moher, D. (2021). The PRISMA 2020 statement : an updated guideline for reporting systematic reviews. *BMJ*, n71. doi : 10.1136/bmj.n71.

Rachavelpula, S. V. R. (2021). *Modelling and Control of Tumbleweed Spherical Rover*. (Thèse de doctorat, Ann Arbor).

Rigatos, G., Busawon, K., Pomares, J. & Abbaszadeh, M. (2019). Nonlinear optimal control for a spherical rolling robot. *International Journal of Intelligent Robotics and Applications*, 3(2), 221–237. doi : 10.1007/s41315-018-0078-2.

Roozegar, M. & Mahjoob, M. J. (2017). Modelling and control of a non-holonomic pendulum-driven spherical robot moving on an inclined plane : simulation and experimental results. *IET CONTROL THEORY AND APPLICATIONS*, 11(4), 541–549. doi : 10.1049/iet-cta.2016.0964.

Roozegar, M., Mahjoob, M. J. & Jahromi, M. (2016). Optimal motion planning and control of a nonholonomic spherical robot using dynamic programming approach : simulation and experimental results. *Mechatronics*, 39, 174–184. doi : 10.1016/j.mechatronics.2016.05.002.

Roozegar, M., Ayati, M. & Mahjoob, M. J. (2017). Mathematical modelling and control of a nonholonomic spherical robot on a variable-slope inclined plane using terminal sliding mode control. *NONLINEAR DYNAMICS*, 90(2), 971–981. doi : 10.1007/s11071-017-3705-9.

Roozegar, M., Mahjoob, M. J. & Ayati, M. (2018). Adaptive tracking control of a nonholonomic pendulum-driven spherical robot by using a model-reference adaptive system. *JOURNAL OF MECHANICAL SCIENCE AND TECHNOLOGY*, 32(2), 845–853. doi : 10.1007/s12206-018-0135-z.

Roy Chowdhury, A., Soh, G. S., Foong, S. H. & Wood, K. L. (2017). Experiments in Second Order Sliding Mode Control of a CPG based Spherical Robot**This work is supported by the Future Systems and Technology Directorate (FSTD), under the Ministry of Defense, Government of Singapore, under Grant IGDST1301013 for Systems Technology for Autonomous Reconnaissance and Surveillance (STARS) project. *20th IFAC World Congress*, 50(1), 2365–2372. doi : 10.1016/j.ifacol.2017.08.426.

Sadeghian, R. & Masouleh, M. T. (2016). Controller tuning based on optimization algorithms of a novel spherical rolling robot. *Journal of Mechanical Science and Technology*, 30(11), 5207–5216. doi : 10.1007/s12206-016-1038-0.

Sadeghian, R., Bayani, H. & Masouleh, M. T. (2015). *Design of an adaptive sliding mode controller for a novel spherical rolling robot*. The Institute of Electrical and Electronics Engineers, Inc. (IEEE) Conference Proceedings. Institute of Electrical and Electronics Engineers Inc. Repéré à http://dx.doi.org/10.1109/ICRoM.2015.7367839.

Sakalli, A., Beke, A. & Kumbasar, T. (2018). Analyzing the Control Surfaces of Type-1 and Interval Type-2 FLCs through an Experimental Study. *The Institute of Electrical and Electronics Engineers, Inc. (IEEE) Conference Proceedings*, 1–6.

Salemizadeh, Parizi, M., Salemizadehparizi, F., Vanaei, S., Karimi, A. & Komijani, H. (2021). Hybrid super-twisting fractional-order terminal sliding mode control for rolling spherical robot. *Asian Journal of Control*, 23(5), 2343–2358. doi : https://doi.org/10.1002/asjc.2696.

Sandino, L. A., Bejar, M. & Ollero, A. (2013). A Survey on Methods for Elaborated Modeling of the Mechanics of a Small-Size Helicopter. Analysis and Comparison. *Journal of Intelligent & Robotic Systems*, 72(2), 219–238. doi : 10.1007/s10846-013-9821-y.

Schroll, G. C. (2009). Angular momentum torque enhancement for spherical vehicles. US.

Schroll, G. C. (2010). *Dynamic Model of a Spherical Robot from First Principles*. Colorado State University. Libraries.

Sugiyama, Y. & Hirai, S. (2006). Crawling and jumping by a deformable robot. *International Journal of Robotics Research*, 25(5-6), 603–620. doi : 10.1177/0278364906065386.

Sun, H. (2021). A High-speed Motion Control Method of Pendulum Driven Spherical Robot. *The Institute of Electrical and Electronics Engineers, Inc. (IEEE) Conference Proceedings*, 1–7. doi : 10.1109/ICAICA52286.2021.9498264.

Tafrishi, S. A., Svinin, M., Esmaeilzadeh, E. & Yamamoto, M. (2019). Design, Modeling, and Motion Analysis of a Novel Fluid Actuated Spherical Rolling Robot. *Journal of Mechanisms and Robotics*, 11(4). doi : 10.1115/1.4043689.

Tang, Y., Liu, J., Liang, J., Yang, T., Xu, K., He, J. & Gao, B. (2021). Co-Simulation of Two-Wheel Differential Spherical Robot Based on ADAMS and MATLAB. *The Institute of Electrical and Electronics Engineers, Inc. (IEEE) Conference Proceedings*. doi : 10.1109/CYBER53097.2021.9588231.

Urakubo, T., Osawa, M., Tamaki, H., Tada, Y. & Maekawa, S. (2012). Development of a spherical rolling robot equipped with a gyro. (2012 IEEE International Conference on Mechatronics and Automation, ICMA 2012), 1602–1607. doi : 10.1109/ICMA.2012.6284376.

Urakubo, T., Monno, M., Maekawa, S. & Tamaki, H. (2016). Dynamic Modeling and Controller Design for a Spherical Rolling Robot Equipped with a Gyro. *IEEE Transactions on Control Systems Technology*, 24(5), 1669–1679. doi : 10.1109/TCST.2015.2508008.

van Eck, N. J. & Waltman, L. (2017). VOSviewer Manual. 49.

Volosyak, I. & Schmidt, M. (2019). Asynchronous control of a spherical robot by means of SSVEP-based brain-computer interface. *7th IEEE International Conference on E-Health and Bioengineering, EHB 2019, November 21, 2019 - November 23, 2019*, (2019 7th E-Health and Bioengineering Conference, EHB 2019). doi : 10.1109/EHB47216.2019.8969955.

Wait, K. W., Jackson, P. J. & Smoot, L. S. (2010). Self locomotion of a spherical rolling robot using a novel deformable pneumatic method. pp. 3757–3762. doi : 10.1109/ROBOT.2010.5509314.

Wang, C.-H., Lin, Y.-H., Huang, K.-S., Lee, B.-K., Lin, K.-B. & Hwang, A. (2011). Constant speed VSC of a spherical robot driven by Omni wheels. 3(Proceedings - International Conference on Machine Learning and Cybernetics), 1214–1219. doi : 10.1109/ICMLC.2011.6016886.

Wang, Y., Guan, X., Hu, T., Zhang, Z., Wang, Y., Wang, Z., Liu, Y. & Li, G. (2021). Fuzzy PID Controller Based on Yaw Angle Prediction of a Spherical Robot. pp. 3242–3247. doi : 10.1109/IROS51168.2021.9636425.

Wang, Y., Liu, Y., Guan, X., Hu, T., Zhang, Z., Wang, Y., Hao, J. & Li, G. (2023). Robust servo linear quadratic regulator controller based on state compensation and velocity feedforward of the spherical robot : Theory and experimental verification. *International Journal of Advanced Robotic Systems*, 20(2). doi : 10.1177/17298806231153229.

Xing, H., Guo, S., Shi, L., Hou, X., Liu, Y. & Liu, H. (2020). Design, modeling and experimental evaluation of a legged, multi-vectored water-jet composite driving mechanism for an amphibious spherical robot. *Microsystem Technologies*, 26(2), 475–487. doi : 10.1007/s00542-019-04536-7.

Ylikorpi, T. J., Halme, A. J. & Forsman, P. J. (2017). Dynamic modeling and obstacle-crossing capability of flexible pendulum-driven ball-shaped robots. *Robotics and Autonomous Systems*, 87, 269–280. doi : 10.1016/j.robot.2016.10.019.

Yu, T., Sun, H., Jia, Q. & Zhao, W. (2013). Path following control of a spherical robot rolling on an inclined plane. *Sensors and Transducers*, 21(SPEC.ISS.5), 42–47.

Yue, M. & Liu, B. Y. (2012). Disturbance adaptive control for an underactuated spherical robot based on hierarchical sliding-mode technology. *PROCEEDINGS OF THE 31ST CHINESE CONTROL CONFERENCE*, pp. 4787–4791.

Yue, M., Liu, B. Y., An, C. & Sun, X. J. (2014a). Extended state observer-based adaptive hierarchical sliding mode control for longitudinal movement of a spherical robot. *NONLINEAR DYNAMICS*, 78(2), 1233–1244. doi : 10.1007/s11071-014-1511-1.

Yue, M., Liu, B. Y., Wei, X. & Hu, P. (2014b). Adaptive Sliding-Mode Control of Spherical Robot with Estimated Rolling Resistance. *CYBERNETICS AND SYSTEMS*, 45(5), 407–417. doi : 10.1080/01969722.2014.919205.

Zadeh, F. K., Moallem, P., Asiri, S. & Zadeh, M. M. (2014). *LQR motion control and analysis of a prototype spherical robot*. The Institute of Electrical and Electronics Engineers, Inc. (IEEE) Conference Proceedings. Institute of Electrical and Electronics Engineers Inc. Repéré à http://dx.doi.org/10.1109/ICRoM.2014.6991017https://www.proquest.com/conference-papers-proceedings/lqr-motion-control-analysis-prototype-spherical/docview/1687415696/se-2?accountid=27231https://etsmtl.on.worldcat.org/atoztitles/link?sid=ProQ:&issn=&volu.

Zhai, Y., Ding, Z., Liu, Y., Jin, S. & Kang, L. (2020). Research on novel spatial structure of power generation of spherical robot. *Proceedings of the Institution of Mechanical Engineers, Part E : Journal of Process Mechanical Engineering*, 234(6), 600–612. doi : 10.1177/0954408920932358.

Zhai, Y., Li, M., Luo, J., Zhou, Y. & Liu, L. (2015). Research of the motion balance of spherical mobile robot based on fuzzy control. *JOURNAL OF VIBROENGINEERING*, 17(1), 13–23.

Zhan, Q., Cai, Y. & Yan, C. (2011). Design, analysis and experiments of an omni-directional spherical robot. *Proceedings - IEEE International Conference on Robotics and Automation*, pp. 4921–4926. doi : 10.1109/ICRA.2011.5980491.

Zhang, L. & Ren, X. (2022). Motion Direction Control of a Spherical Robot. *2021 Chinese Intelligent Systems Conference, 16-17 Oct. 2021*, vol.III(Proceedings of 2021 Chinese Intelligent Systems Conference. Lecture Notes in Electrical Engineering (805)), 786–93. doi : $10.1007/978-981-16-6320-8_81$.

Zhang, L., Ren, X. & Zheng, D. (2023). Modeling and Control of a New Spherical Robot with Cable Transmission. *International Journal of Control, Automation and Systems*, 21(3), 963–974. doi : 10.1007/s12555-021-0936-9.

Zhang, L. F., Ren, X. M. & Guo, Q. (2021). Balance and velocity control of a novel spherical robot with structural asymmetry. *INTERNATIONAL JOURNAL OF SYSTEMS SCIENCE*. doi : 10.1080/00207721.2021.1933253.

Zhang, L., Ren, X. & Zheng, D. (2022). Adaptive Uncertainty Estimator-Based Sliding Mode Control for a Spherical Robot : Methodology and Verification. *Journal of Computational and Nonlinear Dynamics*, 17(10). doi : 10.1115/1.4054593.

Zhang, Q., Jia, Q., Sun, H., Gong, Z. & IEEE. (2009). Application of a Genetic Algorithm-based PI Controller in a Spherical Robot. pp. 180-+.

Zhao, B., Li, M., Yu, H., Hu, H. & Sun, L. (2010). Dynamics and motion control of a two pendulums driven spherical robot. *IEEE/RSJ 2010 International Conference on Intelligent Robots and Systems, IROS 2010 - Conference Proceedings*, pp. 147–153. doi : 10.1109/IROS.2010.5651154.

Zhao, L. & Yu, T. (2014). A new decoupled sliding mode control approach for the linear motion of a spherical rolling robot. *Computer Modelling and New Technologies*, 18(11), 1326–1329.

Zheng, M., Zhan, Q., Liu, J. & Cai, Y. (2011). Control of a spherical robot : Path following based on nonholonomic kinematics and dynamics. *Chinese Journal of Aeronautics*, 24(3), 337–345. doi : 10.1016/S1000-9361(11)60040-X.

Zheng, Y. L., Hu, X. Y. & Sun, H. X. (2021). Research on Motion Control for a Mobile Robot Using Learning Control Method. *APPLIED MATHEMATICS AND NONLINEAR SCIENCES*, 6(1), 227–234. doi : 10.2478/AMNS.2021.1.00038.

Zhou, M., Hou, X., Yin, H., Li, A., Xia, D., Li, Z., Liu, M., Guo, S., Hou, X., Yin, H., Li, A., Xia, D., Li, Z. & Liu, M. (2021). *Trajectory Tracking Control for a Biomimetic Spherical Robot Based on ADRC*. The Institute of Electrical and Electronics Engineers, Inc. (IEEE) Conference Proceedings. Institute of Electrical and Electronics Engineers Inc. Repéré à http://dx.doi.org/10.1109/ICMA52036.2021.9512570.